

Article

Climate Change Impact on Three Important Species of Wild Fruit Forest Ecosystems: Assessing Habitat Loss and Climatic Niche Shift

Facheng Guo, Yaru Yang and Guizhen Gao *

College of Forestry and Landscape Architecture, Xinjiang Agricultural University, Urumqi 830052, China; oooriiii@outlook.com (F.G.); yang042819@163.com (Y.Y.)

* Correspondence: gaogz@xjau.edu.cn; Tel.: +86-15599817032

Abstract: As global biodiversity hotspots, wild fruit forests play key ecological functions, providing essential ecosystem services such as carbon storage, soil retention, and water conservation, and support food chains and biodiversity conservation through key species. Climate change, with rising temperatures and altered precipitation patterns, threatens wild fruit forests by reducing the habitats and numbers of key species, potentially turning these ecosystems from carbon sinks to sources and diminishing overall biodiversity and ecosystem services. However, research on how these changes affect important species' habitats and carbon dynamics remains insufficient. To address this, we analysed habitat suitability for three important species (*Prunus armeniaca* L., *Malus sieversii*, and *Prunus ledebouriana* (Schltdl.) Y.Y.Yao) with the aim of informing conservation strategies. We used biomod2 to integrate environmental and species data using six methods, encompassing 12 models. We predicted overlapping geographical distributions of three species, analysing their ecological niches and environmental interactions using global datasets to understand their adaptations. This analysis revealed ecological niche shifts and reductions in resource utilisation in both current and future scenarios. Their distribution centres will move poleward under the influence of bioclimatic factors and human activities. In conclusion, protecting *P. armeniaca*, *M. sieversii*, and *P. ledebouriana* is essential for the conservation and overall health of wild fruit forest ecosystems. This study provides new insights into climate change, habitat loss, informing conservation and resilience strategies.



Citation: Guo, F.; Yang, Y.; Gao, G. Climate Change Impact on Three Important Species of Wild Fruit Forest Ecosystems: Assessing Habitat Loss and Climatic Niche Shift. *Forests* **2024**, *15*, 1281. <https://doi.org/10.3390/f15081281>

Academic Editor: Dominick A. DellaSala

Received: 29 June 2024

Revised: 12 July 2024

Accepted: 20 July 2024

Published: 23 July 2024



Copyright: © 2024 by the authors. Licensee MDPI, Basel, Switzerland. This article is an open access article distributed under the terms and conditions of the Creative Commons Attribution (CC BY) license (<https://creativecommons.org/licenses/by/4.0/>).

Keywords: climate change; ensemble model; habitat loss; *Prunus armeniaca* L.; *Malus sieversii*; *Prunus ledebouriana* (Schltdl.) Y.Y.Yao

1. Introduction

The Earth is currently undergoing its sixth mass extinction, primarily driven by habitat fragmentation due to degradation and loss, with climate change being a major factor [1–3]. The Intergovernmental Panel on Climate Change (IPCC) reports a significant increase of 1.1 °C in average global surface temperature from 2011 to 2020 compared with pre-industrial levels [4]. This increase, which is linked to escalating greenhouse gas emissions from human activities, has exacerbated global warming. The combined effects of global warming and other stressors significantly impact terrestrial ecosystems, altering their structure and function and causing shifts in species habitats and distributions [5,6]. Habitat fragmentation further disrupts interspecies interactions, increases vulnerability, and leads to widespread extinction and extirpation [7–9].

Vegetation is crucial as both an indicator and component of climate response, with species survival depending on genetic diversity, adaptability to environmental changes, and migration to suitable climates [10,11]. Species in fragmented or rare habitats face higher risks of migration difficulties or extinction [12,13]. Climate is a key determinant of species distribution, and changes in distribution patterns are clear indicators of climate shifts [14,15]. The complex relationships among climate change, human disturbances, and

biodiversity conservation present a multifaceted challenge [16,17]. Forests cover a third of the Earth's land area and are vital for global carbon sequestration, holding 56% of terrestrial ecosystem carbon [18]. Trees absorb significant carbon dioxide through photosynthesis and store it in biomass, litter, deadwood, and soil organic matter. Natural forests, unlike simpler artificial forests, are more effective in biodiversity conservation and provide key ecosystem services, such as carbon storage, soil retention, and water conservation [19].

The wild fruit forest region, identified as one of the key biodiversity hotspots worldwide, has garnered widespread academic attention owing to its abundant biological resources and unique ecosystem structure. These forests, which have survived geological changes and climatic variation since the Tertiary Period, serve as sanctuaries for thermophilic mesophytic broadleaf trees. Their existence is a result of their unique geological history and local climate conditions of warmth and humidity, in contrast to early desert climates [20,21]. However, climate change, overgrazing, tourism, and unsustainable harvesting have severely affected these habitats, causing a drastic reduction in their area and number [22,23]. Key species such as *Prunus armeniaca* L., *Malus sieversii*, and *Prunus ledebouriana* (Schltdl.) Y.Y.Yao, all Tertiary relicts, are the dominant species in these wild fruit forests [24–28]. *M. sieversii*, the ancestor of modern apples, is native to the Tianshan Mountains, including the regions within China, Kazakhstan, and Kyrgyzstan [20]. *P. armeniaca*, from the Rosaceae family, has played a crucial role in the history of cultivated apricots and is prominent in Xinjiang's wild fruit forests [20,26]. *P. ledebouriana*, also in the Rosaceae family, now exists only in relict distributions in Kazakhstan and Xinjiang, China, with notable fossilisation in Europe [29–31]. The loss of habitats for these three keystone species will directly result in a reduction in biodiversity in the wild fruit forests, which, in turn, will have a negative impact on ecosystem functions and stability. It also affects the continuation of breeding and conservation programs. Understanding the potential overlapping geographical distributions of these species, along with their ecological niche dynamics and conservation area planning, is essential for their utilisation and protection against habitat loss due to climate change.

Species Distribution Models (SDMs) are crucial for predicting how climate change affects important species by integrating environmental data and species occurrences to forecast their potential geographic distributions [32–37]. Common SDMs, such as the maximum entropy model (Maxent), CLIMEX, generalised linear model (GLM), and genetic algorithm for rule-set prediction (GARP), are widely used to predict the distribution of important species, weeds, biocontrol agents, disease vectors, and pathogens [38,39]. Biomod, an R-based SDM platform developed in 2003 and now updated to biomod2 [40], provides a range of algorithms, including artificial neural networks (ANNs), classification tree analysis (CTA), flexible discriminant analysis (FDA), generalized additive models (GAMs), gradient boosting machines (GBMs), generalized linear models (GLMs), multivariate adaptive regression splines (MARSs), maximum entropy (MAXENT), MAXNET, random forest (RF), species range envelope (SRE), and eXtreme Gradient Boosting (XGBOOST) [41], for predicting species distributions, while ensemble models (EMs) are increasingly favoured for their ability to separate signal from noise in individual SDMs, avoid exposing vulnerabilities to species limitations, enhancing the reliability of geographical distribution predictions [42–46]. The 'ecospat' package effectively integrates environmental principal component analysis (PCA-env) to streamline ecological niche dynamic analysis. This integration ensures a more coherent and efficient workflow [47,48]. Introduced in 2014, the COUE (centroid shift, overlap, unfilling, and expansion) framework has gained widespread application in examining the dynamics of species' ecological niches. This approach is notably applied in research focused on *Ambrosia artemisiifolia* L., commonly known as common ragweed, and *Agastache rugosa*, a significant cash crop [49–51].

Our hypotheses focused on the direct impacts of climate change, specifically, the effects of rising temperatures and altered precipitation patterns on the habitats of three important species: *P. armeniaca*, *M. sieversii*, and *P. ledebouriana*. We predicted that increasing global temperatures and more frequent extreme climatic events will significantly reduce suitable

habitats for these species, compress their ecological niches, and decrease the area and biodiversity of wild fruit forests. To predict the future geographic distribution of these important species, we employed SDMs, integrating existing distribution data with future climate projections to estimate likely survival areas. We chose climatic factors—temperature, precipitation, and seasonal variation—and non-climatic factors like soil type and topography to define current ecological niches and project how future climate changes might alter species distributions. Our methodology included the following: (1) selecting high-precision individual models for each species in biomod2 after simulation testing; (2) EM application to forecast possible distribution zones and intersecting areas in both current and future climate conditions, specifically targeting the 2050s and 2090s periods; (3) analysis of ecological niche overlap and dynamics among these species, particularly between native and habitat loss areas; (4) identifying environmental variables that significantly impact their potential distributions; and (5) using the Marxan model to identify priority conservation areas and suitable growth environments. The study primarily aimed to provide a scientific basis for conserving wild populations and germplasm resources of these species.

2. Methods

2.1. Data on the Geographical Spread of Target Species

Our research gathered worldwide location records for three important species, *P. armeniaca*, *M. sieversii*, and *P. ledebouriana*. We analysed these data using a comprehensive checklist of SDMs [52]. Initially, we searched online databases for the geographical distribution data of these species. Specifically, for *P. armeniaca*, *M. sieversii*, and *P. ledebouriana*, we obtained 110, 484, and 19 records from the Global Biodiversity Information Facility (<http://www.gbif.org/>, accessed 28 July 2023), and 11, 7, and 10 records from the Chinese Virtual Herbarium (<http://www.cvh.ac.cn>, accessed 28 July 2023), respectively. In addition, 21, 25, and 17 records were sourced from the literature [24–28]. We excluded distribution records that were assigned to capital cities or based on the centroids of provinces. Furthermore, we included records from the Center for Agriculture and Bioscience International (<https://www.cabi.org/>, accessed 28 July 2023) and conducted country-based extrapolation. In enhancing the precision of environmental variables, only one distribution point was maintained per 10×10 km grid, employing ENMTools [53]. This process led to the aggregation of 383 location records across the three species (275 for *P. armeniaca*, 79 for *M. sieversii*, and 36 for *P. ledebouriana*), as shown in Figure 1.

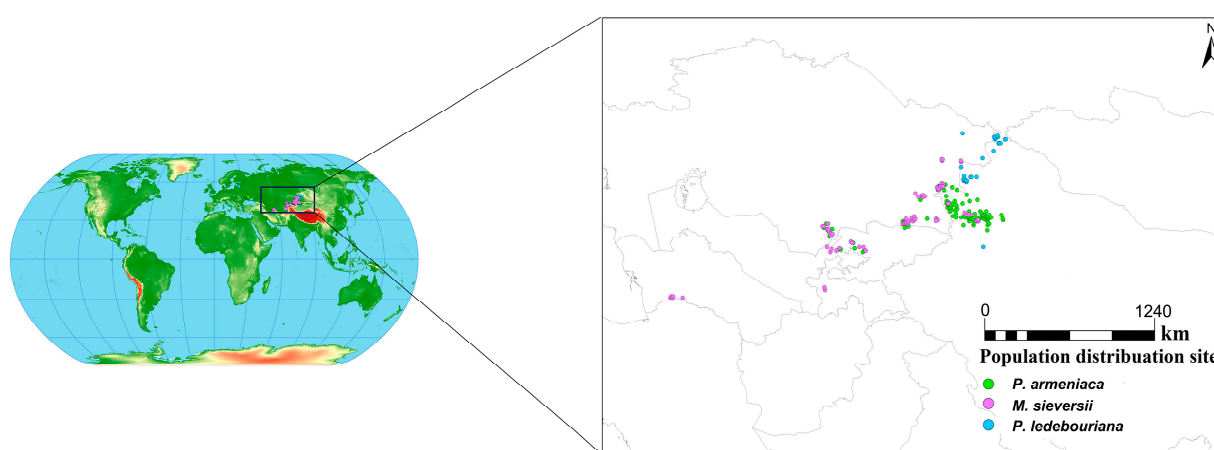


Figure 1. Geographical distribution records of *Prunus armeniaca*, *Malus sieversii*, and *Prunus ledebouriana*.

2.2. Environmental Variables

This study incorporated 39 environmental factors, including 19 bioclimatic, 3 topographic, and 17 soil factors (Table 1). From the Paleoclim database (<http://www.paleoclim.org>, accessed 29 July 2023), we acquired raster files of 19 bioclimatic variables, each at a 5 arcmin resolution. These variables, originating from detailed monthly records of temperature

and precipitation, have formed a globally utilised dataset for ecological studies, spanning from 1979 to 2013. For projections of future climates, specifically the periods 2041–2060 (the 2050s) and 2081–2100 (the 2090s), data were retrieved from the Worldclim2.1 database (<http://www.worldclim.org/>, accessed 29 July 2023). Each of these periods included 19 climate factors named bio1–bio19 [54]. Future climate scenarios were selected from the sixth phase of the International Coupled Model Intercomparison plan (CMIP6). This approach differs from the typical concentration pathway (RCP) scenario used in CMIP5, which combines different shared socioeconomic paths (SSPs) with RCPs, and incorporates aspects of future socioeconomic development. We chose three combined scenarios, SSP1-2.6, SSP2-4.5, and SSP5-8.5, representing low, medium, and high radiation forcing scenarios, respectively. The spatial resolution of these data was 2.5 arcmin (~5 km). Soil-related parameters originated from the World Soil Database (HWSD), courtesy of the Science Data Center of Cold and Arid Regions. Topographic information was sourced from a geospatial data cloud (<http://www.gscloud.cn/>, accessed 29 July 2023). The prediction of suitable habitats was based on the premise that soil and topographic conditions will remain unchanged for the forthcoming 70 years [55].

The analysis of the 37 environmental factors (excluding soil and topographic factors) employed Pearson correlation and the variance inflation factor (VIF) to assess their correlation and significance. In the R language, we conducted Spearman’s correlation and multicollinear VIF evaluations on the point interpolation data. Initially, we filtered out factors showing correlations of <0.8 and VIF values of <10. VIF, also known as the reciprocal of tolerance, indicates the degree of multicollinearity, where VIF < 10 indicates no multicollinearity, VIF > 10 < 100 indicates multicollinearity, and VIF > 100 indicates serious interfactor multicollinearity. The filtered modelling factors are shown in Table 1.

Table 1. Participation modelling environment variables.

Environmental Factors	Variable Name	Work Unit	<i>P. armeniaca</i>	<i>M. sieversii</i>	<i>P. ledebouriana</i>
Bioclimatic factors	Annual Mean Temperature	°C	√	√	
	Mean Diurnal Range	°C			
	Isothermality	%	√		√
	Temperature Seasonality	°C			√
	Max Temperature in Warmest Month	°C			
	Min Temperature in Coldest Month	°C			
	Temperature Annual Range	°C			
	Mean Temperature in Wettest Quarter	°C			√
	Mean Temperature in Driest Quarter	°C			√
	Mean Temperature in Warmest Quarter	°C			
	Mean Temperature in Coldest Quarter	°C			
	Annual Precipitation	mm			
	Precipitation in Wettest Month	mm	√	√	√
	Precipitation in Driest Month	mm		√	
	Precipitation Seasonality	%	√	√	√
	Precipitation in Wettest Quarter	mm			
	Precipitation in Driest Quarter	mm			
Precipitation in Warmest Quarter	mm	√	√		
Precipitation in Coldest Quarter	mm	√	√		
Topographic factors	elevation	M	√	√	√
	aspect	A	√	√	√
	slope	S	√	√	√

Table 1. Cont.

Environmental Factors	Variable Name	Work Unit	<i>P. armeniaca</i>	<i>M. sieversii</i>	<i>P. ledebouriana</i>
Soil factors	USDA Texture Class			√	
	Topsoil Effective Thickness	cm			
	Topsoil Texture Class				
	Topsoil Reference Bulk Density	g/cm ³			
	Topsoil Silt Content	%			
	Topsoil pH	0–14			
	Topsoil Organic Carbon	%	√		√
	Topsoil Gravel Content	%			√
	Topsoil Exchangeable Sodium Percentage	%	√	√	
	Topsoil Electrical Conductivity of the Extract	dS/m			√
	Topsoil Clay Content	%		√	
	Topsoil Cation Exchange Capacity of the Soil	meq/100 g			
	Topsoil Cation Exchange Capacity of the Clay	meq/100 g			
	Topsoil Calcium Carbonate Equivalent	%	√	√	
	Topsoil Calcium Carbonate	%			
	Topsoil Bulk Density	g/cm ³			
Topsoil Base Saturation	%	√		√	
Human	Human_foot		√	√	√

2.3. SDM Development and Accuracy Assessment

Our research involved modelling the present and anticipated future geographic distributions of three important species (*P. armeniaca*, *M. sieversii*, and *P. ledebouriana*) utilising global occurrence data alongside environmental variables. This process was facilitated through the biomod2 package within R Studio [56]. In biomod2, we applied a suite of 12 distinct algorithms, specifically, ANN, CTA, FDA, GAM, GBM, GLM, MARS, MAXENT, MAXNET, RF, XGBOOST, and SRE. For each of these species, a random selection of 75% of their distribution records constituted the training dataset; the remaining 25% formed the test dataset [57]. To increase the models' reliability, we repeated this distribution segmentation five times.

Additionally, we generated 1000 pseudo-absence points, repeating this step three times to refine our models. Consequently, 360 models were developed. Through accuracy assessment, we selected four models that consistently showed average values exceeding 0.9 for further analysis. These models included ANN, CTA, FDA, GAM, GBM, GLM, MARS, MAXENT, MAXNET, RF, and XGBOOST.

We constructed an EM using 11 individual models, employing six integration methods: EMmean, EMcv, EMci, EMmedian, EMca, and EMwmean. The EM was used to predict the potential geographical distributions of *P. armeniaca*, *M. sieversii*, and *P. ledebouriana*. For assessing the accuracy of the model, the true skill statistic (TSS) and area under the receiver operating characteristic curve (ROC–AUC) were employed. The ROC curve compares the false-positive rate (1 – specificity) to the true-positive rate (1 – omission rate) [58]. The TSS metric, which measures the average omission error, is independent of the size of the verification dataset and combines the benefits of the kappa statistic (occurrence, sensitivity, and specificity) without frequency dependence [59]. Higher TSS and AUC values indicate better model accuracy. In the suitability zoning phase, the biomod2 model results were integrated into ArcGIS to produce raster data. The predicted suitability zones for the three species were classified into four grades: high suitability (0.66–1), medium suitability (0.33–0.66), low suitability (0.05–0.33), and unsuitable (0–0.05) [60].

2.4. Geographical Distribution Migration and Overlaps

We employed the SDM tool, which was integrated into the ArcGIS software (version 10.4), to examine potential shifts in the geographical distributions of three important species under various climate scenarios. Following the methodology outlined by Brown (2014), we mapped the distribution of these species using the SDM tool (available at <http://www.sdmtoolbox.org>, accessed on 1 September 2023). Our analysis focused on the changes in their distributional centroids, which were assessed based on a suitability threshold. Specifically, habitats with a probability of >0.3 were classified as 'suitable', while those with a probability of 0.3 or less were considered 'unsuitable'.

We employed the Centroid Changes (Lines) tool from the SDM Toolbox (v2.4) to analyse the migration of potential geographic distribution centres using binarised rasters. Initially, the rasters representing the geographic distributions of the three important species were scaled by factors of 1, 2, and 4 using ArcGIS 10.4's (Environmental Systems Research Institute, Inc. RedLands, CA, USA) Raster Calculator. These scaled rasters were then aggregated to delineate the overlapping distribution areas of the species. This step is crucial for identifying regions in which multiple species converge, indicating a heightened invasive risk. The identification of these common areas is vital for developing targeted conservation strategies to protect ecosystems from the potential impacts of these important species.

2.5. Measurement of Ecological Niches

We quantitatively analysed the ecological niches of *P. armeniaca*, *M. sieversii*, and *P. ledebouriana* across different periods and under various climatic conditions. Initially, we compared the ecological niche dynamics between native areas and regions facing habitat loss, utilising occurrence and bioclimatic data with the R Studio (Version 4.2.3, Molly Hill, NJ, USA) ecospat package [61,62]. This approach utilised the PCA-env and COUE methods to conduct a comprehensive analysis of the bioclimatic variables associated with the species [48,49].

We then performed climate niche similarity tests between native areas and those experiencing habitat loss, using the ecospat package with 1000 repetitions for each test [63]. A significant difference in ecological niche similarity values ($p < 0.05$) indicated ecological niche dissimilarity.

Furthermore, using the ecospat package, we analysed and visualised the ecological niches of the species, including computing the ecological niche overlap index, 'D'. This index ranged from 0 (no overlap) to 1 (complete overlap), representing the extent of ecological niche overlap. We also used the ENMTool niche breadth module to calculate ecological niche breadths based on current and future potential distribution data [64]. Here, 'B1' denotes the minimum and 'B2' denotes the maximum niche breadth.

2.6. Marxan Model Construction

The Marxan model, known for its effectiveness in identifying minimum-cost areas for conservation planning [65,66], was used to identify priority conservation areas for *P. armeniaca*, *M. sieversii*, and *P. ledebouriana* under current climatic conditions. Owing to continuous improvements, this model has become popular for land conservation planning. It operates at a spatial resolution of 2 km² using square planning units (PUs), each measuring 25,000 m in height and width. In ArcGIS, we used the 'Zonal Statistics as Table' tool to aggregate species distribution data within each PU, which helped us construct a species distribution matrix.

We set a conservation target that includes 30% of the total habitat area, applying a species protection factor (SPF) of 100. A crucial aspect of the Marxan model is its boundary length modifier (BLM), which was set at 25,000. The BLM acts as a correction parameter for the perimeter of a conservation area [67]. By adjusting the BLM, we analysed the balance between the cost, total boundary length, and area. Such an analysis is essential for determining the equilibrium point that leads to a more efficient spatial distribution pattern

in conservation areas [68]. To ensure the reliability of our findings, the model was run over 100 iterations to determine the optimal configuration of the planning units.

3. Results

3.1. Model Precision Assessment

We assessed the accuracy of various models, including ANN, CTA, FDA, GAM, GBM, GLM, MARS, MAXENT, MAXNET, RF, XGBOOST, and SRE, and the EM for *P. armeniaca*, *M. sieversii*, and *P. ledebouriana*. For these species, the TSS values of the CTA, FDA, GAM, GBM, GLM, MARS, MAXENT, MAXNET, RF, and XGBOOST models were >0.8, and their AUC values were >0.9 (Figure 2). Consequently, 10 models with high accuracy were chosen to construct EMs using six different integration methods: EMmean, EMcv, EMci, EMmedian, EMca, and Emwmean.

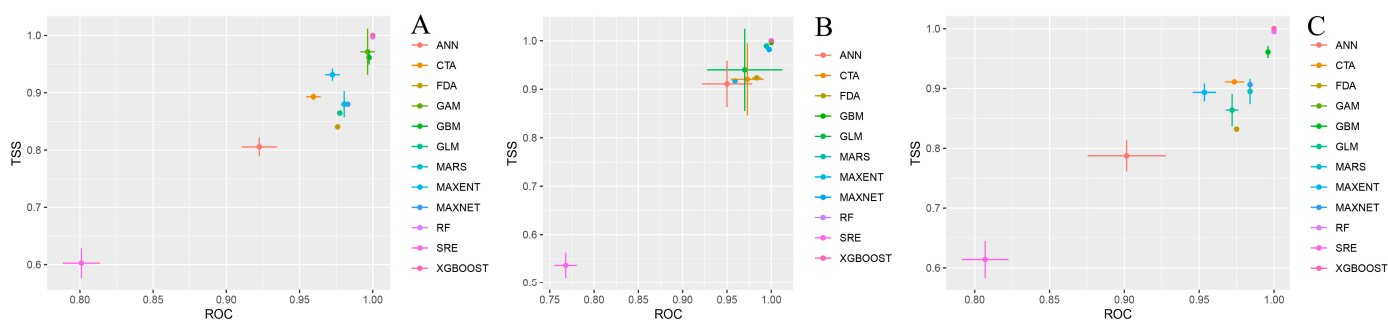


Figure 2. Evaluation indices of individual predictive models (AUC: area under the receiver operating characteristic, TSS: true skill statistic, ANN: artificial neural network, CTA: classification tree analysis, FDA: flexible discriminant analysis, GAM: generalised additive model, GBM: generalised boosting model, GLM: generalised linear model, MARS: multivariate adaptive regression spline, MAXENT: maximum entropy, MAXNET: Maxent’s network equivalent, RF: random forest, XGBOOST: eXtreme gradient boosting, SRE: surface range envelope) for distribution of three plants, (A) *Prunus armeniaca*, (B) *Malus sieversii*, and (C) *Prunus ledebouriana*.

The developed EMs demonstrated the highest accuracy in this assessment. For *P. armeniaca*, *M. sieversii*, and *P. ledebouriana*, the TSS values of the EMs were 0.92, and the AUC values were up to 0.98 (Figure 3). Hence, the EMs developed from singular high-precision models significantly enhanced the fit accuracy while diminishing uncertainties in the fitting process. This suggests a high reliability in the predicted potential geographic distributions of the three important species, as inferred through the use of EMs.

3.2. Present Potential Geographic Spread

The EM projections of the current (1979–2013) potential geographic ranges for *P. armeniaca*, *M. sieversii*, and *P. ledebouriana* are shown in Figure 4. *P. armeniaca* and *M. sieversii* share common distribution zones in Armenia, Azerbaijan, China, Iran, Italy, Kazakhstan, Turkey, and Kyrgyzstan, while *P. ledebouriana* is primarily native and endemic to Kazakhstan. Notably, the shared areas in China, Kazakhstan, and Turkey represent 73.38% of the total joint distribution for *P. armeniaca* and *M. sieversii*. China has the largest shared area, at 8.76×10^6 ha, accounting for 37.32% of the total, followed by Kazakhstan (27%, 6.34×10^6 ha) and Turkey (9.05%, 2.12×10^6 ha) (Table 2). The largest global habitat suitability area for *P. ledebouriana* is significantly concentrated in Kazakhstan (979.17×10^6 ha), followed by the global habitat suitability areas for *M. sieversii* (468.20×10^6 ha) and *P. armeniaca* (445.51×10^6 ha).

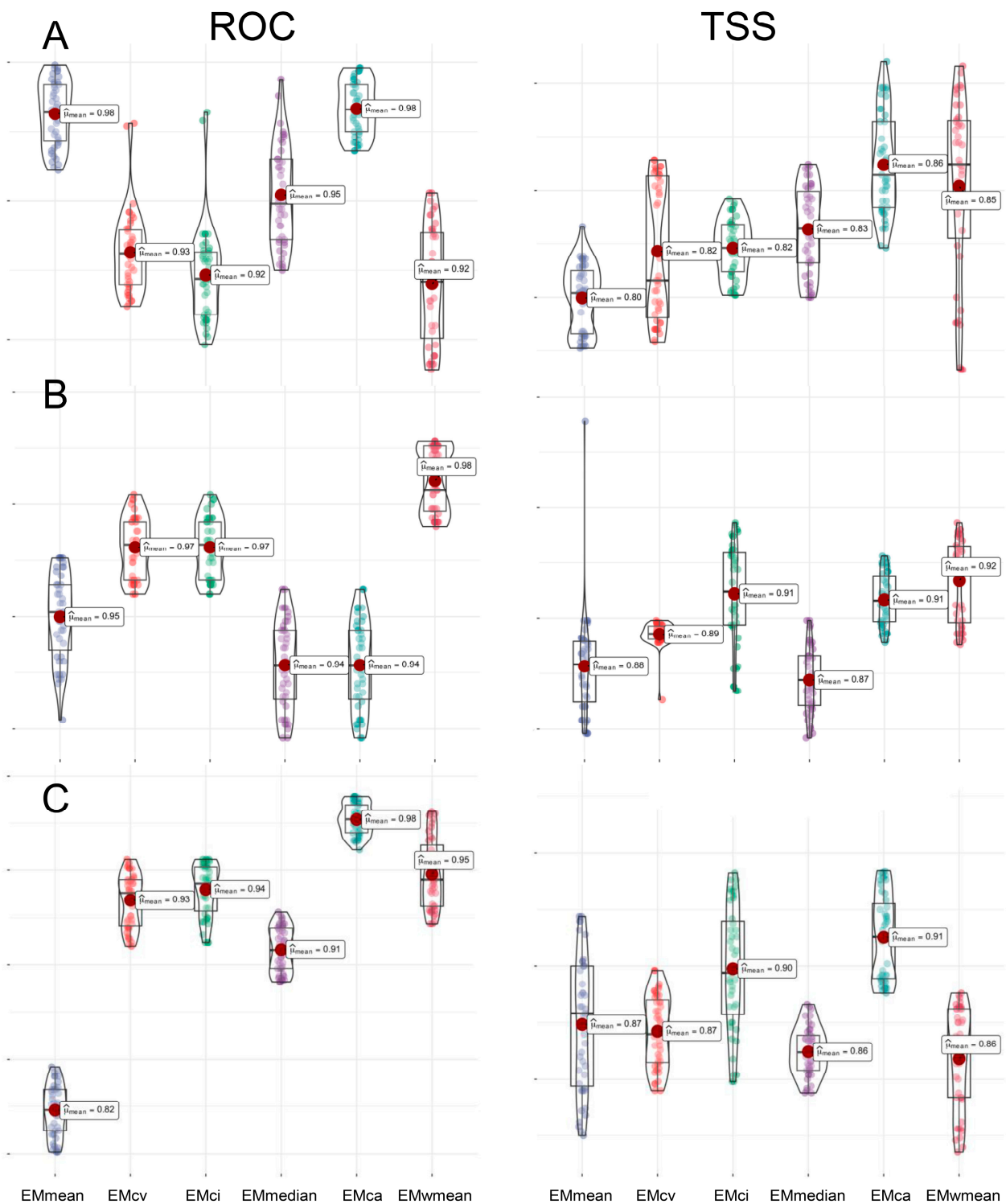


Figure 3. Six integration methods (EMmean: ensemble mean, EMcv: ensemble coefficient of variation, EMci: ensemble confidence interval, EMmedian: ensemble median, EMca: ensemble concordance analysis, EMwmean: ensemble weighted mean) under the integrated model score. (A) *Prunus armeniaca*, (B) *Malus sieversii*, and (C) *Prunus ledebouriana*.

P. armeniaca has a highly suitable habitat spread over 151.14×10^6 ha, predominantly in Europe (Ukraine, Romania, Russia), Central Asia (Kazakhstan, Turkmenistan, Pakistan, northwestern China), and North America (United States, southern Canada), with sparse distribution in Oceania (Australia). Eastern Europe is the main area of the most suitable

habitat for *P. armeniaca*, accounting for 70.4% of the total suitable area, followed by Central Asia and North America with 21.89% and 0.44%, respectively (Table 3). For *M. sieversii*, highly suitable habitats, covering 121.99×10^6 ha, are mainly in Central Asia (Mongolia, Iran, Turkey, Kazakhstan, Kyrgyzstan, Tajikistan, Turkmenistan, northwestern China), Europe (Georgia, Spain), Africa (Morocco, Algeria, Swaziland), South America (Chile, Argentina, Trinidad, and Tobago), and North America (United States, southern Canada). The highly suitable habitat of *M. sieversii* is concentrated in Central Asia with 56.05%, followed by North America (16.39%), Africa (10.32%), Europe (6.31%), and South America (6.31%) (Table 4). For *P. ledebouriana*, highly suitable habitats span 468.86×10^6 ha, predominantly in Europe (Azerbaijan, Ukraine, Russia, Romania, Bulgaria, Germany), Central Asia (Kyrgyzstan, Kazakhstan, Iran, Turkey, northwestern China), and North America (United States, southern Canada). The main habitat of *P. ledebouriana* is located in Europe, which accounts for 60.51% of the total area, while Central Asia and North America account for 19.66% and 11.89%, respectively (Table 5).

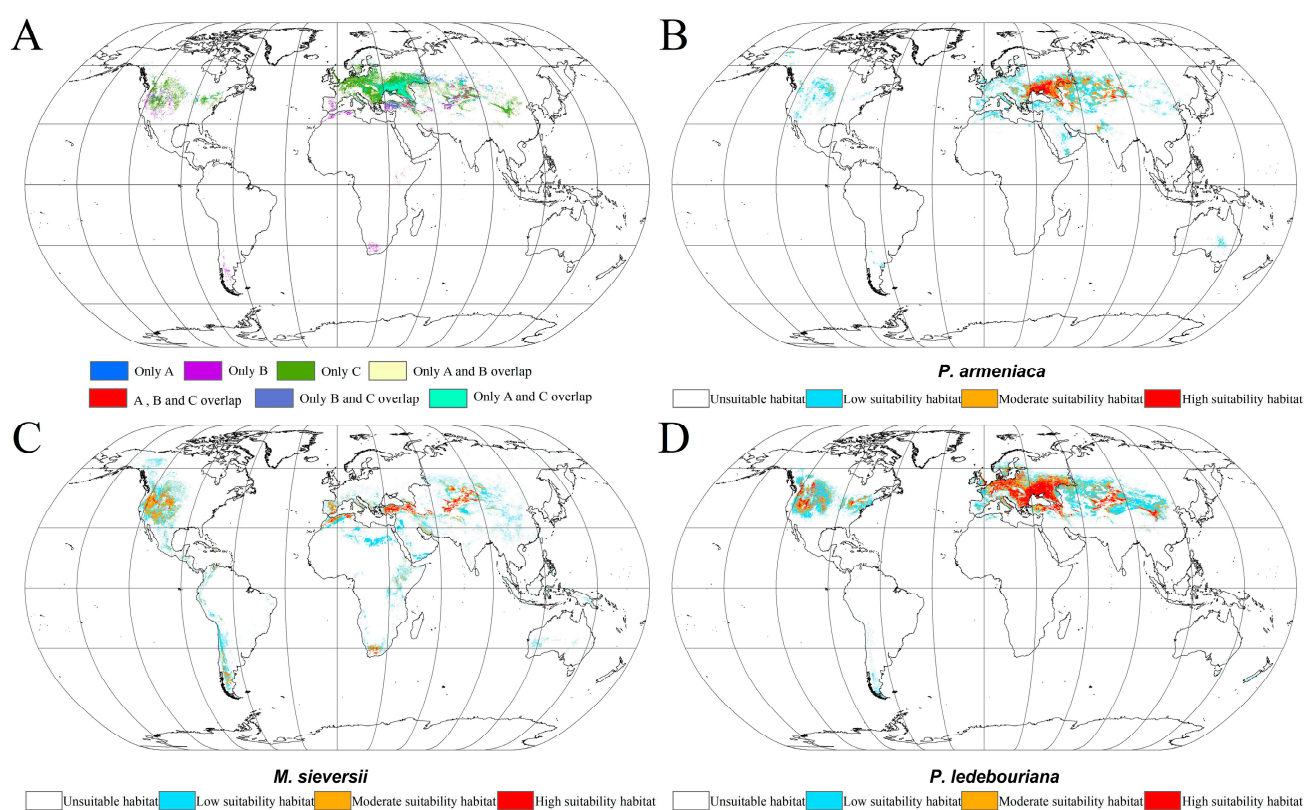


Figure 4. Current global geographical distributions of *Prunus armeniaca*, *Malus sieversii*, and *Prunus ledebouriana* predicted using the EM. (A) Overlay zones, (B) *P. armeniaca*, (C) *M. sieversii*, and (D) *P. ledebouriana*.

Table 2. Area of overlap under the current climate conditions.

Overlap Zone	Area ($\times 10^6$ ha)
Armenia	1.64
Azerbaijan	1.67
China	8.76
Iran	1.55
Italy	0.28
Kazakhstan	6.34
Turkey	2.12
Kyrgyzstan	1.08

Table 3. Global distribution of *Prunus armeniaca* under current climate scenarios ($\times 10^6$ ha).

Habitability Classification	Distribution Area		
	European	Asian	North American
Highly suitable habitat	106.41	33.09	0.68
Moderately suitable habitat	92.94	1225.11	12.42

Table 4. Global distribution of *Malus sieversii* under current climate scenarios ($\times 10^6$ ha).

Habitability Classification	Distribution Area				
	Asian	European	African	North American	South American
Highly suitable habitat	68.38	7.70	12.60	20.00	2.43
Moderately suitable habitat	86.71	18.29	29.45	143.95	20.60

Table 5. Global distribution of *Prunus ledebouriana* under current climate scenarios ($\times 10^6$ ha).

Habitability Classification	Distribution Area		
	Asian	European	North American
Highly suitable habitat	92.19	283.73	55.76
Moderately suitable habitat	138.84	199.58	118.79

3.3. Comparative Analysis of Ecological Niches

The geographic ranges of these three important species partially mirror their fundamental niches, defined as the array of environmental conditions allowing their survival. The ecological niche dynamics of *M. sieversii*, *P. armeniaca*, and *P. ledebouriana*, based on a comparison of the climate niche space between native and lost habitats, are presented in Figure 5. Based on occurrence data and bioclimatic variables for native and habitat loss, the ecological niche overlaps of *P. armeniaca*, *M. sieversii*, and *P. ledebouriana* revealed Schoener's D values of 0.83, 0.74, and 0.76, respectively, indicating that the ecological niche overlap is relatively high between *P. armeniaca*, *M. sieversii*, and *P. ledebouriana* (Figure 5). The ecological niches of *P. armeniaca*, *M. sieversii*, and *P. ledebouriana* in their extirpated habitats were smaller than those in their native habitats. This indicates a decrease in resources that can be jointly utilised in both the current and future periods. In terms of habitat loss, the ecological niches of *P. armeniaca*, *M. sieversii*, and *P. ledebouriana* did not occupy all the ecological niches of their native areas. The null hypothesis of the ecological niche equivalence of *P. armeniaca*, *M. sieversii*, and *P. ledebouriana* based on the bioclimatic variables of the native and invasive areas was not rejected ($p = 0.1908$, 0.9523 , and 0.5238 , respectively).

The niche widths of *P. armeniaca*, *M. sieversii*, and *P. ledebouriana* were calculated using the ENMTools (Version 5.26) software package, focusing on various climate conditions. As shown in Table 6, the B1 and B2 values of *P. armeniaca*, *M. sieversii*, and *P. ledebouriana* were all >0.7 and >0.9 , respectively. Hence, each period showed no marked distinction between B1 and B2, suggesting that *P. armeniaca*, *M. sieversii*, and *P. ledebouriana* tend towards being generalist species. Furthermore, B1 and B2 exhibited an upward trend in alternative climate scenarios compared with the present period. This trend implies an expansion in the range of resources utilised by these species in forthcoming climate conditions, demonstrating their extensive distribution and robust environmental adaptability.

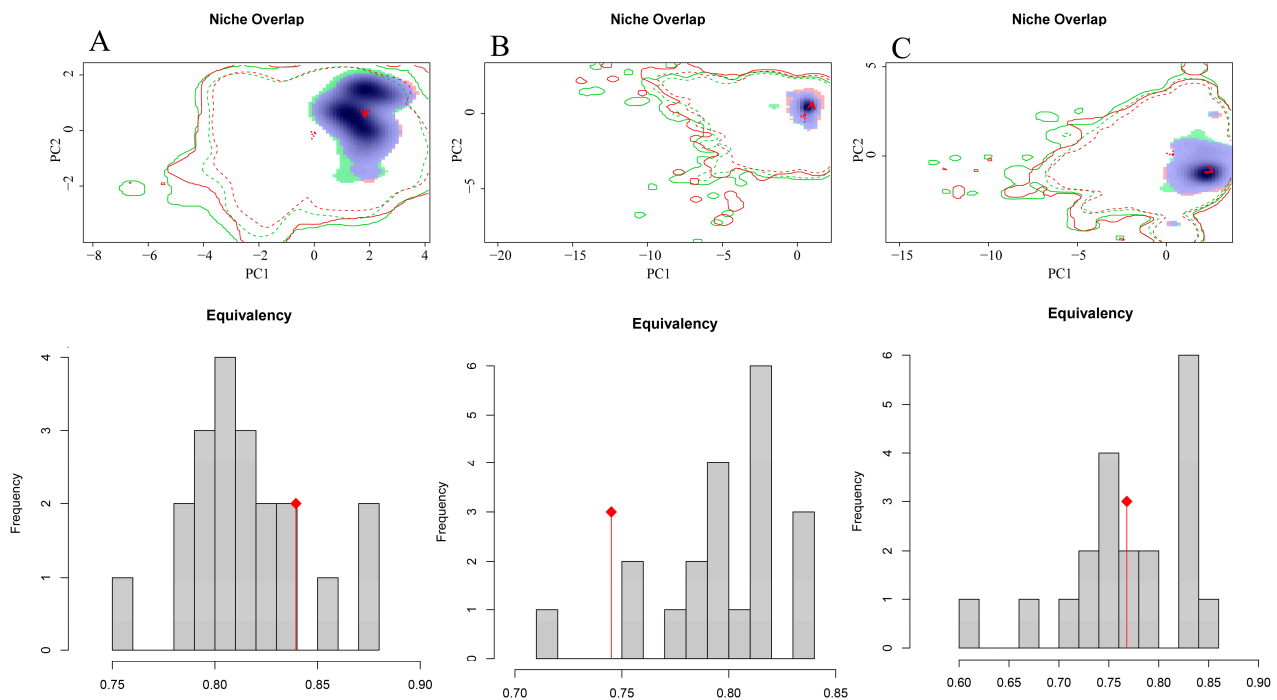


Figure 5. Niche differences in *Prunus armeniaca* (A), *Malus sieversii* (B), and *Prunus ledebouriana* (C) in the future.

Table 6. Niche widths for three important species.

Species	Climate Scenario	B1 (Minimum Ecotope)	B2 (Maximum Ecotope Width)
<i>P. armeniaca</i>	Current	0.8560	0.9958
	2050s_SSP126	0.8585	0.9959
	2050s_SSP245	0.8563	0.9958
	2050s_SSP585	0.8595	0.9960
	2090s_SSP126	0.8580	0.9959
	2090s_SSP245	0.8634	0.9961
	2090s_SSP585	0.9035	0.9973
	<i>M. sieversii</i>	Current	0.8569
2050s_SSP126		0.8589	0.9959
2050s_SSP245		0.8582	0.9958
2050s_SSP585		0.8584	0.9958
2090s_SSP126		0.8609	0.9959
2090s_SSP245		0.8592	0.9959
2090s_SSP585		0.8631	0.9960
<i>P. ledebouriana</i>	Current	0.7766	0.9927
	2050s_SSP126	0.8279	0.9943
	2050s_SSP245	0.8254	0.9943
	2050s_SSP585	0.8307	0.9944
	2090s_SSP126	0.8294	0.9944
	2090s_SSP245	0.8228	0.9942
	2090s_SSP585	0.8248	0.9942

3.4. Projected Future Geographic Ranges

The potential global geographical distributions of *P. armeniaca*, *M. sieversii*, and *P. ledebouriana* under SSP126, SSP245, and SSP585 during the 2050s and 2090s are shown in Figures 6–8 and Table 7.

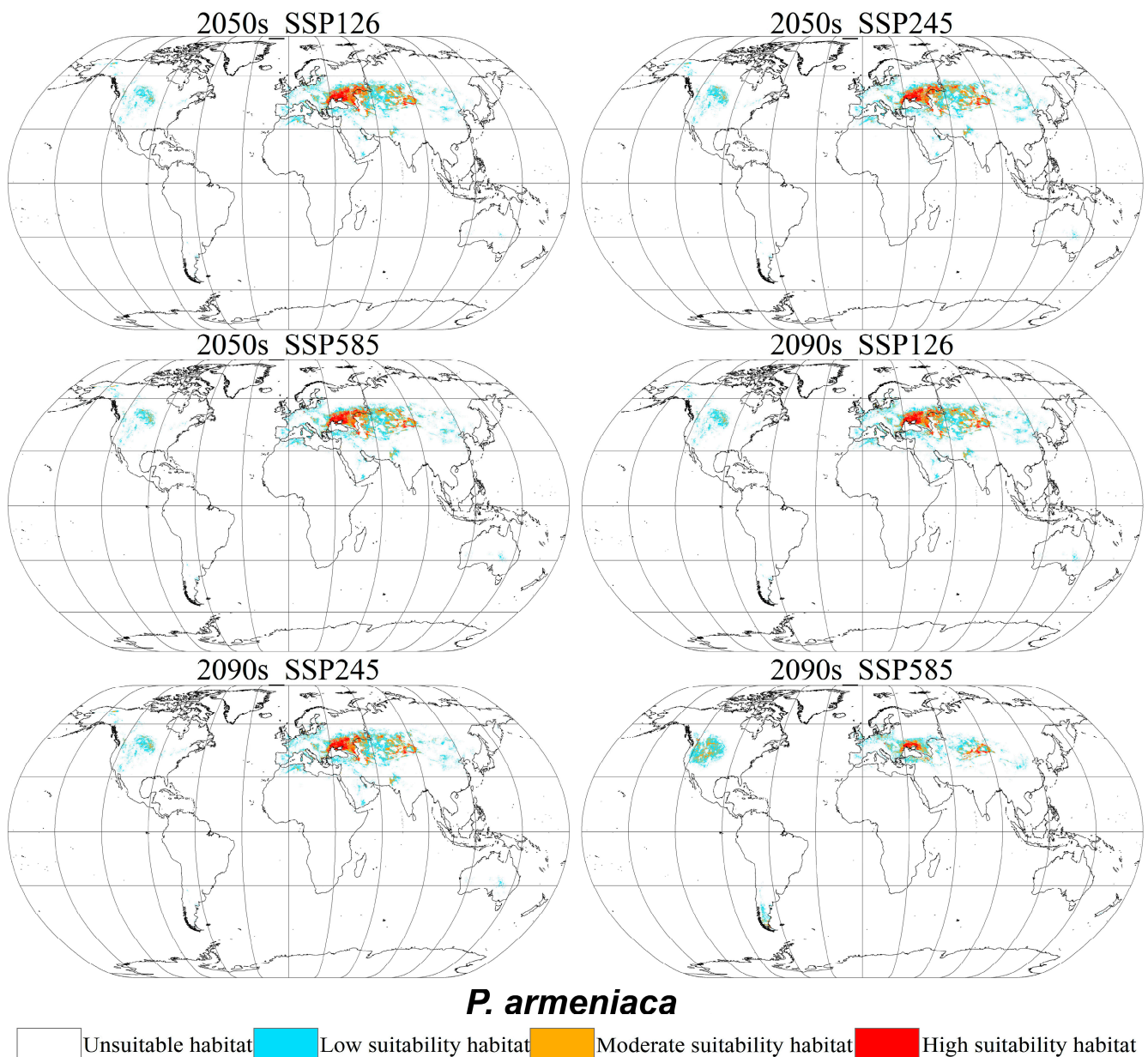


Figure 6. Potential global geographical distribution of *Prunus armeniaca* in the 2050s and 2090s predicted using the ensemble model (EM). The scenarios include SSP126, SSP245, and SSP585.

For *P. armeniaca*, the total area of suitable habitat is projected to decrease under most future climate scenarios in the 2050s and 2090s. The most significant reduction occurs in the 2090s under the SSP585 scenario, with the suitable habitat area decreasing to 885×10^6 ha, representing a 32.21% reduction from current conditions. Habitat losses are primarily noted in Romania, Ukraine, southern Russia, and sporadically across Central Asia, although some expansions are noted in Central Asia and southern Europe.

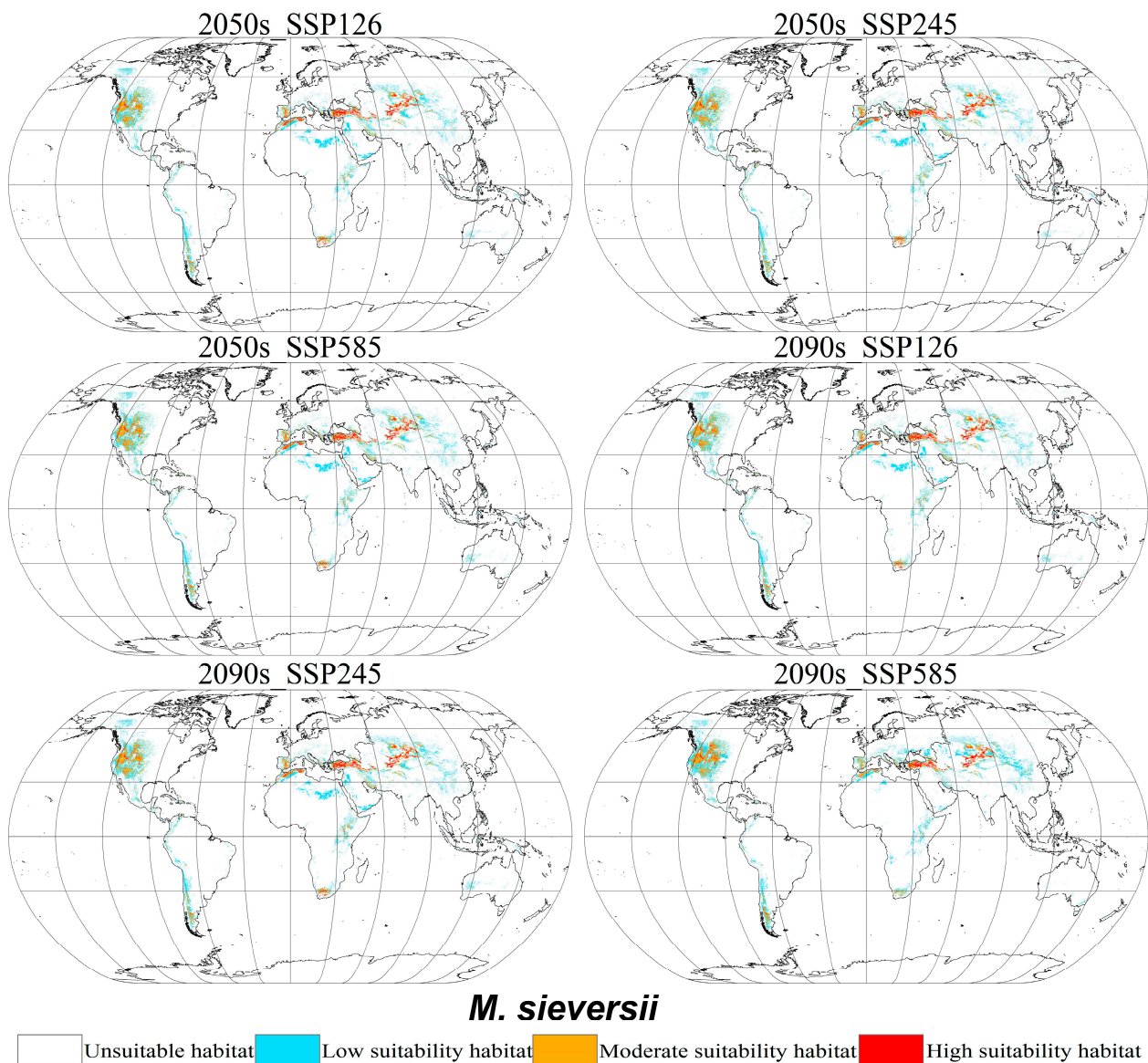


Figure 7. Potential global geographical distribution of *Malus sieversii* in the 2050s and 2090s predicted using the ensemble model (EM). The scenarios include SSP126, SSP245, and SSP585.

For *M. sieversii*, the total area of suitable habitat is projected to decrease under all climate scenarios in the 2050s and 2090s compared with current conditions. The most significant loss occurs in the 2090s under the SSP585 scenario, with the suitable habitat area decreasing to 1389×10^6 ha, a 3.71% reduction. Habitat losses are mainly in Romania, Ukraine, southern Russia, and sporadically in Central Asia, although some habitat expansions are observed mainly in Central Asia, with a few in southern Europe. Other notable reductions include the SSP126 scenario in the 2090s with a 3.34% reduction, followed by the SSP245 scenario in the 2050s and the SSP126 scenario in the 2050s with smaller decreases.

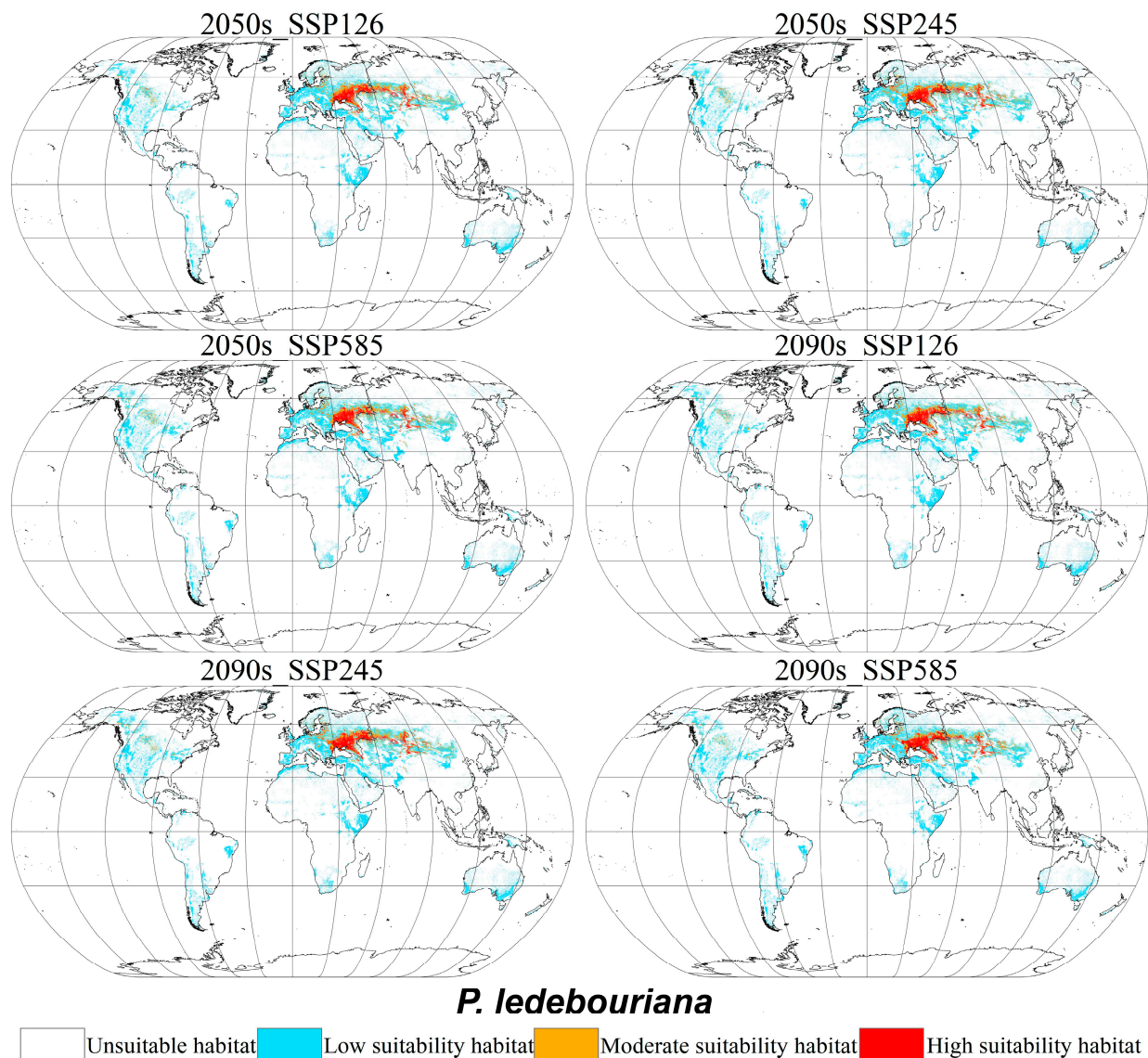


Figure 8. Potential global geographical distribution of *Prunus ledebouriana* in the 2050s and 2090s predicted using the ensemble model (EM). The scenarios include SSP126, SSP245, and SSP585.

For *P. ledebouriana*, the total area of suitable habitat is expected to decrease under all future climate scenarios in the 2050s and 2090s compared with current conditions. The most significant loss is forecasted for the 2050s under the SSP585 scenario, with the suitable habitat area reducing to 517.95 million ha, a 47.1% decrease. The primary habitat losses are noted along the borders of Ukraine, Russia, and Georgia, with smaller affected areas in Kazakhstan, Mongolia, and northwestern China. Some habitat expansions are observed in Moldova and limited areas of southwestern Russia. Other significant reductions are projected under the SSP126 scenario in the 2090s with a 46.68% decrease, the SSP585 scenario in the 2090s with a 45.13% decrease, and the SSP126 scenario in the 2050s with a 43.99% decrease.

Table 7. Global area of distribution of three important species under future climate scenarios ($\times 10^6$ ha).

Species	Climate Scenario	Habitability Classification			
		None	Low	Medium	High
<i>P. armeniaca</i>	2050S_SSP126	13,457.71	789.38	292.76	146.55
	2090S_SSP126	13,373.77	866.98	306.78	138.88
	2050S_SSP245	14,892.61	852.57	310.77	143.71
	2090S_SSP245	13,439.94	8327.96	2829.22	130.75
	2050S_SSP585	133,473.19	772.36	299.53	141.32
	2090S_SSP585	13,770.01	637.67	188.58	59.29
<i>M. sieversii</i>	2050S_SSP126	13,265.7	968.32	331.62	120.76
	2090S_SSP126	13,291.53	953.39	324.2	117.28
	2050S_SSP245	13,271.8	953.73	339.99	120.88
	2090S_SSP245	13,247.42	970.16	333.71	118.37
	2050S_SSP585	13,264.87	962.12	339.66	119.75
	2090S_SSP585	13,266.02	965.19	311.45	112.89
<i>P. ledebouriana</i>	2050S_SSP126	11,687.41	2423.91	319.06	229.28
	2090S_SSP126	11,817.81	2346.51	292.17	229.9
	2050S_SSP245	11,773.25	2347.44	323.24	242.47
	2090S_SSP245	11,733.88	2385.73	302.2	264.59
	2050S_SSP585	11,771.91	2396.54	297.01	220.94
	2090S_SSP585	11,726.92	2422.26	275.45	261.78

Non: Unsuitable habitat; Low: Low suitability habitat; Medium: Moderate suitability habitat; High: High suitability habitat.

3.5. Overlapping Geographical Distributions under Climate Change

In the future, the primary regions experiencing a loss of overlapping geographic distribution areas for the three important species will mainly be located in Azerbaijan, Georgia, Kazakhstan, Tajikistan, Kyrgyzstan, Iran, and northwestern China, as illustrated in Figure 9. The area of lost overlapping geographic distributions for the three important species was largest for the 2090s under the SSP245 scenario, followed by the 2050s under SSP126, 2050s under SSP245, 2050s under SSP585, 2090s under SSP585, and 2090s under SSP126.

In the 2050s, under the SSP126 scenario, the greatest loss in overlapping geographic distribution areas occurred in Iran, amounting to 108.8×10^4 ha, which represents 31.85% of the total loss in overlapping geographic distribution. This was followed by Kazakhstan (85×10^4 ha, 27.02%) and Georgia (72.25×10^4 ha, 22.97%). Under the SSP245 scenario, Kazakhstan experienced the most significant loss, totalling 67.15×10^4 ha, accounting for 31.71% of the total loss in overlapping areas, followed by Iran (51×10^4 ha, 24.09%) and Kyrgyzstan (46.75×10^4 ha, 22.08%). Under the SSP585 scenario, Iran again suffered the most, with a loss of 54.4×10^4 ha, representing 34.04% of the total, followed by Kyrgyzstan (47.6×10^4 ha, 29.78%) and Azerbaijan (45.05×10^4 ha, 28.19%).

In the 2090s, under the SSP126 scenario, Azerbaijan saw the most significant loss in overlapping geographic distribution areas, with 54.4×10^4 ha lost, accounting for 87.67% of the total loss. This was followed by Kyrgyzstan (38.25×10^4 ha, 61.64%) and Kazakhstan (25.5×10^4 ha, 41.09%). Under the SSP245 scenario, the largest loss occurred in Kazakhstan, with 124.95×10^4 ha, representing 31.68% of the total loss, followed by Iran (11.9×10^4 ha, 30.17%) and Kyrgyzstan (70.55×10^4 ha, 17.88%). Under the SSP585 scenario, Iran again experienced the largest loss, with 50.15×10^4 ha, constituting 43.06% of the total, followed by Kazakhstan (45.9×10^4 ha, 39.41%) and Azerbaijan (36.55×10^4 ha, 31.38%) (Table 8).

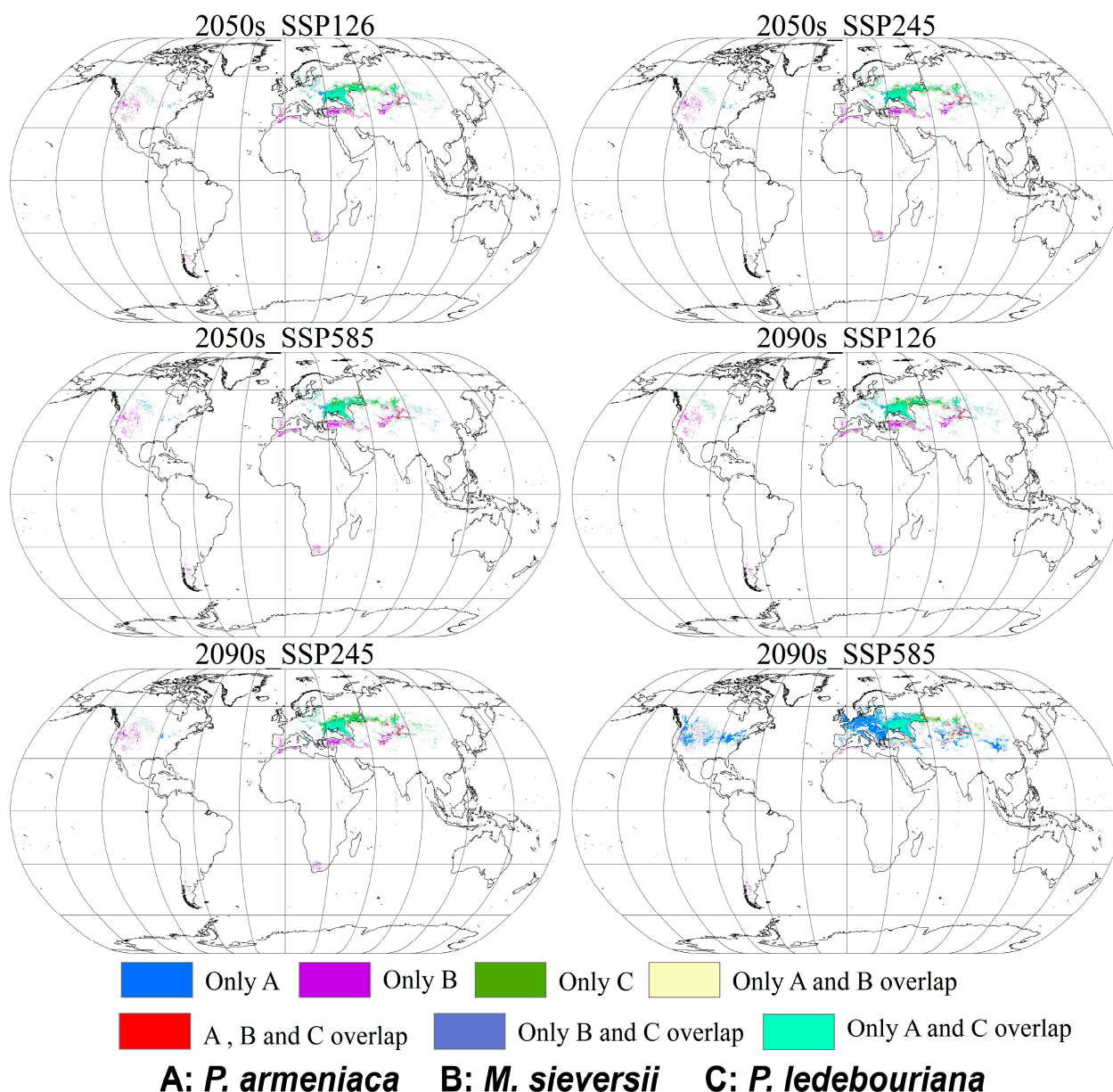


Figure 9. Predicted overlapping geographic ranges of *Prunus armeniaca*, *Malus sieversii*, and *Prunus ledebouriana* in the 2050s and 2090s under SSP126, SSP245, and SSP585.

Table 8. Future overlap zone shrinkage area (km²).

Period	Climate Scenario	Scenario Overlap Zone						
		Azerbaijan	China	Georgia	Iran	Kazakhstan	Kyrgyzstan	Tajikistan
2050s	SSP126	5270	−6800	7225	10,880	8500	5950	425
	SSP245	4250	−680	1615	5100	6715	4675	−510
	SSP585	4505	−1785	1785	5440	2380	4760	−1105
2090s	SSP126	5440	−5440	1615	−1615	2550	3825	−170
	SSP245	6120	510	1445	11,900	12,495	7055	−85
	SSP585	3655	−6035	1530	5015	4590	3060	−170

3.6. Centres of Potential Geographical Distributions

The potential geographic distribution centres of *P. armeniaca*, *M. sieversii*, and *P. ledebouriana* are shown in Figure 10. The centres of potential geographical distributions of *P.*

armeniaca are Friuli-Venezia Giulia, Italy, under current climate scenarios; the centres of potential geographical distributions of *M. sieversii* are Karaman, Turkey, under current climate scenarios; and the centres of potential geographical distributions of *P. ledebouriana* are Vasvar, Vas, Hungary, under current climate scenarios. Under the three scenarios from the present to the 2050s and 2090s, *P. armeniaca* showed an overall trend of moving northward and from northeastern Europe to Central Asia. For *M. sieversii*, from the present to the 2050s and 2090s, the potential geographic distribution centres generally shifted northward and northwestward in Europe, with the centre oscillating under the SSP245 scenario. For *P. ledebouriana*, from the current period to the 2050s and 2090s, the potential geographic distribution centres tended to move northward from northeastern Europe to Central Asia, exhibiting a swaying trend in Central Asia. Overall, the potential geographic distribution centres of these three important species predominantly trend northward under the three scenarios projected for the 2050s and 2090s (Table 9).

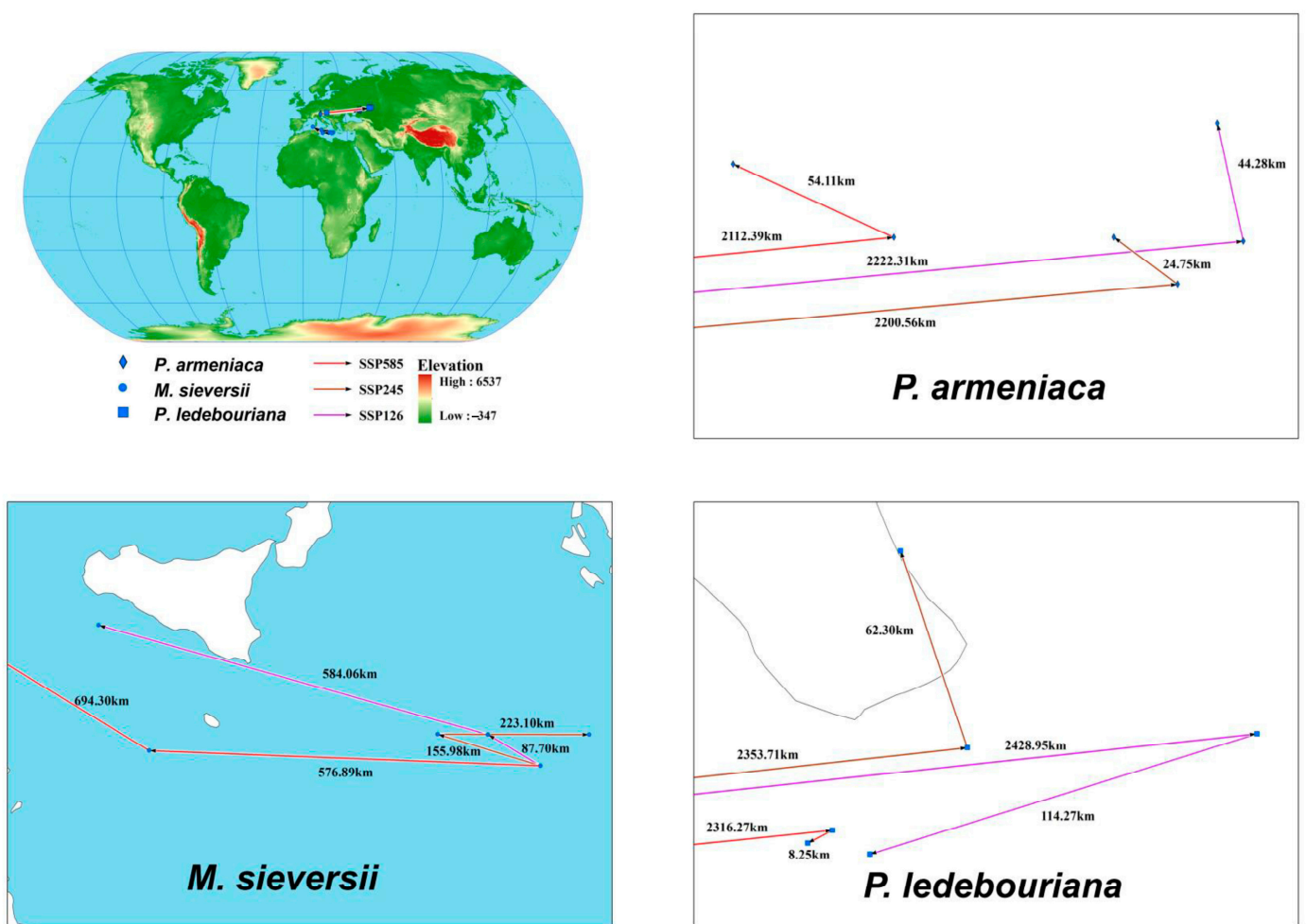


Figure 10. Centroid changes in the distribution of *Prunus armeniaca*, *Malus sieversii*, and *Prunus ledebouriana* in future climate scenarios.

Table 9. The centres of potential geographical distributions of three important species.

Species	Climate Scenario	Distribution		Migration Distance (km)
		Longitude	Latitude	
<i>P. armeniaca</i>	CURRENT	12.4456	46.2602	—
	2050S_SSP126	41.9697	48.4101	2222.31
	2090S_SSP126	41.9545	48.8085	44.28
	2050S_SSP245	41.6546	48.2651	2200.56
	2090S_SSP245	41.4184	48.4232	24.75
	2050S_SSP585	40.4762	48.4232	2112.39
	2090S_SSP585	39.8432	48.6712	54.11
<i>M. sieversii</i>	CURRENT	19.7714	35.2959	—
	2050S_SSP126	18.9452	35.7089	87.70
	2090S_SSP126	12.6646	37.1596	584.06
	2050S_SSP245	18.1248	35.7124	155.98
	2090S_SSP245	20.5975	35.7089	223.10
	2050S_SSP585	13.4065	35.4970	576.89
	2090S_SSP585	6.76638	38.8237	694.30
<i>P. ledebouriana</i>	CURRENT	16.9523	47.0332	—
	2050S_SSP126	49.8891	49.7767	2428.95
	2090S_SSP126	48.3927	49.4345	114.27
	2050S_SSP245	48.8311	49.7373	2353.71
	2090S_SSP245	48.7509	50.2956	62.30
	2050S_SSP585	48.2766	49.5022	2316.27
	2090S_SSP585	48.177	49.4657	8.25

3.7. Influence of Environmental Variables on Predicted Geographic Distributions

We utilised the EMca integrated model to evaluate the impact of each environmental variable on the potential geographic distributions of *P. armeniaca*, *M. sieversii*, and *P. ledebouriana*, as detailed in Figure 11. The analysis revealed that for *P. armeniaca*, annual mean temperature (Bio1), isothermality (Bio3), and precipitation in the wettest month (Bio13) had the most significant cumulative contributions. For *M. sieversii*, the key bioclimatic variables were precipitation in the wettest month (Bio13), driest month (Bio14), warmest quarter (Bio18), and coldest quarter (Bio19). For *P. ledebouriana*, the major contributing variables for *P. ledebouriana* were isothermality (Bio3), precipitation in the wettest month (Bio13), and temperature seasonality (Bio4). These variables predominantly define the multidimensional ecological niche of each species; however, other climatic, soil, and topographic factors play smaller roles.

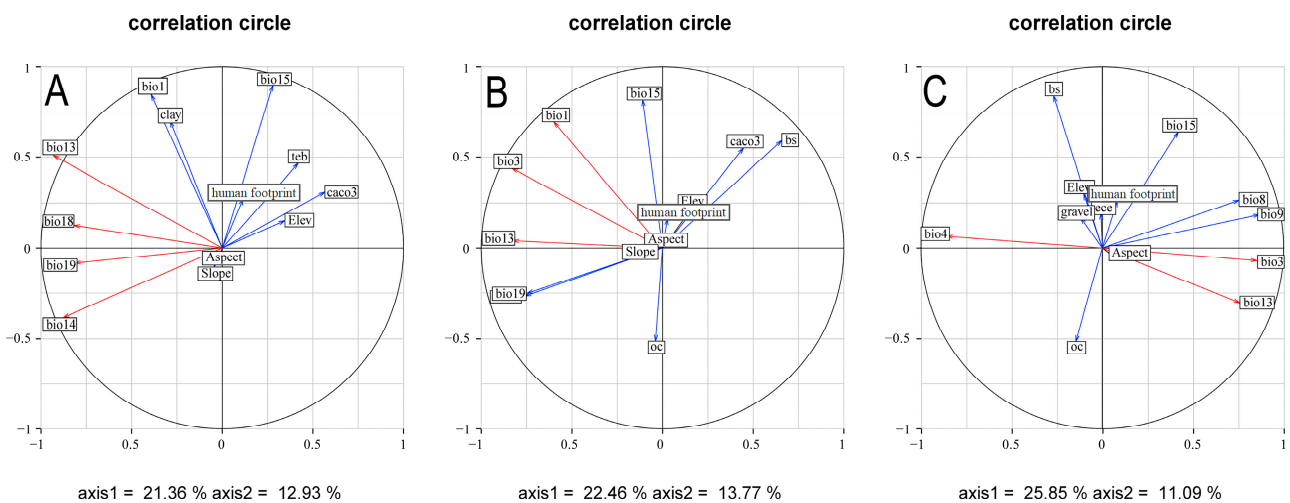


Figure 11. Dominant environmental factors of *Prunus Armeniaca* (A), *Malus sieversii* (B), and *Prunus Ledebouriana* (C).

3.8. Priority Protection Areas under Current Climate Conditions

The Marxan model was employed to identify priority conservation areas for the three important species, with the findings imported into ArcGIS to develop a focused conservation strategy. As depicted in Figure 12, these priority areas are predominantly located in Armenia, Azerbaijan, China, Iran, Italy, Kazakhstan, Turkey, and Kyrgyzstan. This distribution aligns with the highly suitable habitats for these species as forecasted by the biomod2 model, affirming the precision of these predictions. Furthermore, these crucial conservation zones cover a relatively small portion of the land, exhibiting a compact distribution. This is beneficial for establishing specific conservation and management plans.



P. armeniaca* *M. sieversii* *P. ledebouriana **Priority area**

Figure 12. Global priority conservation areas for *Prunus armeniaca*, *Malus sieversii*, and *Prunus ledebouriana* as predicted by the Marxan model.

4. Discussion

4.1. Influences of Environmental Data and Spatial Resolutions on SDM Efficacy

Beyond bioclimatic factors, a range of elements can affect the performance of SDMs [69], including topographic features and human impacts [70,71], which play distinct roles in determining species distributions. In this study, climate, soil, digital elevation model (DEM), and habitat integrity index (HII) data were integrated into the SDMs to project the global distribution patterns of the three important species, with a focus on prediction accuracy [51]. We utilised environmental data of varying resolutions. However, existing studies suggest that increased spatial resolution does not necessarily enhance SDM predictive accuracy. Therefore, to reduce uncertainties linked to disparate spatial resolutions in environmental data, we normalised the resolution of all the environmental variables.

4.2. Importance of Predictions by EMs

Individual SDMs are often used to predict species colonisation and extinction; however, they can suffer from overfitting or inadequacy [72]. EMs, which combine multiple SDM predictions, offer greater accuracy and reduced uncertainty, making them ideal for forecasting the potential geographic distributions of important and endangered species under various conditions, such as climate change and human impacts [34,35,73]. In this study, 11 individual SDMs (ANN, CTA, FDA, GAM, GBM, GLM, MARS, MAXENT, MAXNET, RF, and XGBOOST) were used to create the EM. Despite the high TSS (>0.8) and AUC (>0.9) values for the individual SDMs, the EM achieved even better scores (>0.92 and >0.98), enhancing the prediction accuracy.

P. armeniaca, *M. sieversii*, and *P. ledebouriana* are vital for the stability and ecosystem services of wild fruit forests, offering significant genetic resources and insights into plant

evolution. However, their global geographical and niche overlaps remain unexplored. Using the EM in biomod2, we predicted the global potential distribution and niche breadth of these three important species under climate change conditions, evaluating future habitat loss, overlap of lost and native areas, reserve planning, and key environmental variables influencing their distribution. This study provides a comprehensive approach for conserving and utilising similar species globally.

4.3. Response of Spatial Distribution Patterns of Three Important Species to Climate Change

This century, most regions of the northern hemisphere are expected to experience the effects of climate change. Under climate change, species may face three potential outcomes: adapting in place, migrating to track shifting climates spatially or temporally, or facing local extinction [74,75]. Predictions of the potential geographic distribution of vulnerable species under climate change can serve as an early warning signal [76]. This change may cause range dislocations and species turnover, threatening native flora and increasing the risk of extinction [77]. The geographic ranges of *M. sieversii*, *Juglans regia*, *Prunus armeniaca*, *Crataegus chlorocarpa*, *Prunus cerasifera*, and *Sorbus tianschanica* are expected to shrink owing to climate change, leading to a decline in the diversity of wild fruit forests in the Xitianshan Mountains [78]. Furthermore, studies indicate that the geographic range of *M. sieversii* has declined owing to climate change, with nature reserves covering only a small fraction of the remaining suitable areas [79]. A consequence of climate change is the shift of plant communities to higher elevations [80–83] and new dimensions [84,85] to follow favourable climate conditions. This inability to adapt threatens rare species, potentially leading to population declines and eventual extinction [86]. Contrary to previous studies, our research indicates that the geographic ranges of *P. armeniaca*, *M. sieversii*, and *P. ledebouriana* are diminishing owing to climate change, with suitable habitats moving to higher latitudes, thereby increasing the risk of extinction from habitat loss. Our findings corroborate the hypothesis that climate change intensifies habitat loss for important species, enhance our understanding of how global warming influences the geographic shifts of these species, and offer a scientific foundation for devising future conservation strategies.

4.4. Environmental Factors Restricting the Distributions of *P. armeniaca*, *M. sieversii*, and *P. ledebouriana*

Under current climatic conditions, the primary environmental factors affecting the distribution of *P. armeniaca*, *M. sieversii*, and *P. ledebouriana* are temperature and precipitation, followed by topographic factors; soil factors have the least impact on these species. According to the EM model, suitable habitats for *P. armeniaca*, *M. sieversii*, and *P. ledebouriana* are mainly at altitudes of 1000–1400 m, which aligns with their actual living conditions [24,26,27]. Although thermohydric conditions play a major role in the potential global geographic distribution patterns of *P. armeniaca*, *M. sieversii*, and *P. ledebouriana*, the constraints of topography and soil factors should not be overlooked. The contribution rates of environmental factors indicate that a combination of factors, including temperature, moisture, altitude, and slope, will jointly affect the potential geographic distributions of *P. armeniaca*, *M. sieversii*, and *P. ledebouriana*.

4.5. Priority Protection Areas for *P. armeniaca*, *M. sieversii*, and *P. ledebouriana*

Nature reserves are essential to safeguard natural resources and biodiversity. In exploring systematic reserve zoning for *P. armeniaca*, *M. sieversii*, and *P. ledebouriana*, we identified priority conservation areas in Armenia, Azerbaijan, China, Iran, Italy, Kazakhstan, Turkey, and Kyrgyzstan. These countries offer ideal environments for these species largely because of their unique geographical locations and climatic conditions. The regions, which are mainly in temperate to semi-arid climate zones, consist of mountainous and plateau terrains that foster diverse ecological environments [27,87]. This diversity allows species to thrive at various altitudes and microclimates, matching their specific growth habits.

The key growth factors in these areas include ample sunlight, a moderate climate, and balanced moisture. The mountainous regions of Armenia and Azerbaijan offer varied microclimates, whereas plateau areas in Western China and Central Asia provide essential nutrients with unique soil types and textures. The semi-arid climates of Iran and Turkey facilitate efficient water use, whereas the warm climates and good soil drainage of Italy and Kyrgyzstan are beneficial for these species. These conditions not only align with the growth habits of *P. armeniaca*, *M. sieversii*, and *P. ledebouriana*, but also support their biodiversity and genetic diversity. Therefore, these regions are crucial for the growth and conservation of these valuable species and offer significant opportunities for research and preservation.

Furthermore, while in situ conservation within these natural reserves is vital, the importance of ex situ conservation efforts cannot be understated. Ex situ strategies, such as the establishment of seed banks and living collections, play a crucial role in complementing in situ measures by providing a 'safety net' against potential loss of genetic diversity due to environmental or anthropogenic pressures [88,89]. This dual approach ensures the preservation of a genetic reservoir for *P. armeniaca*, *M. sieversii*, and *P. ledebouriana*, which can be crucial for restoration and research purposes under changing global conditions. The integration of ex situ and in situ conservation strategies will therefore enhance our capacity to maintain and recover these species in their natural habitats, while also allowing for controlled scientific studies and breeding programs that can further support their conservation.

4.6. Model Prediction Limitations

This study's modelling and analysis present inherent limitations and challenges. First, the field surveys lacked comprehensiveness, potentially skewing the species distribution data away from typical patterns. This could introduce biases, with notably less thorough surveys in remote and complex terrains compared with more accessible areas. Second, the exclusion of biological factors as predictor variables limited the simulation to theoretical ecological niches, rather than representing the species' actual ecological niches [90,91]. Although the impact of human footprint was considered, urbanisation and deeper anthropogenic influences, which are particularly significant in densely populated areas of Europe and beyond, were not explicitly modelled. This oversight may affect the accuracy of our predictions as urban expansion can alter local ecosystems, climate conditions, and species interactions [92,93]. Extrapolating models to future environmental conditions beyond current training data impacts prediction reliability [94]. Additionally, unmodelled factors such as migration capabilities, barriers, and evolutionary responses to environmental changes could affect species distribution predictions [95]. Therefore, it is crucial to consider these factors when applying predictions to field surveys and conservation efforts [96]. The environmental variables for this study were sourced from the Paleoclim database, covering the period 1979–2013. This range extends nearly a decade beyond the 1950–2000 period available in the WorldClim database [52,74]. However, climate data for the most recent decade remain absent. Consequently, it is essential to include the missing data in future research to enhance the reliability and robustness of the predictions.

5. Conclusions

The potential geographical distributions of *P. armeniaca*, *M. sieversii*, and *P. ledebouriana* are shaped by bioclimatic variables, the HII, soil attributes, and topography, with global climate change significantly impacting their distribution and overlapping areas. Our EM outperformed individual models such as ANN, CTA, FDA, GAM, GBM, GLM, MARS, MAXENT, MAXNET, RF, and XGBOOST, showing that it is more reliable for predicting the geographical distributions of these important species.

The EM predictions showed that these species are primarily distributed in Central Asia and Europe and undergo ecological niche changes during invasion. Under climate scenarios SSP126, SSP245, and SSP585, suitable habitats are projected to decrease by the 2050s and 2090s. In the 2050s, the overlapping geographic distribution areas will mainly be

in Azerbaijan, China, Iran, Kazakhstan, and Georgia. By the 2090s, these areas are expected to shift predominantly to China, Kazakhstan, Kyrgyzstan, and Georgia, with a general trend of moving northward.

Bioclimatic variables and elevation are significant influencers of their distribution, whereas the cumulative impact of topography and soil properties is low. The potential loss of distribution areas for these species is a serious concern, threatening the genetic diversity and adaptability of wild fruit forest ecosystems to environmental change.

In conclusion, the protection of *P. armeniaca*, *M. sieversii*, and *P. ledebouriana* extends beyond biodiversity conservation, and is essential for ecosystem vitality, scientific advancement, and economic resilience. A comprehensive conservation strategy that includes habitat protection, natural reproduction support, and management plans is crucial. This approach, guided by EMs and ecological studies, is the key to preserving biodiversity and ensuring sustainable coexistence in the face of climate change, habitat loss, and carbon sequestration.

Author Contributions: Conceptualisation, G.G., F.G. and Y.Y.; methodology, G.G., F.G. and Y.Y.; software, Y.Y.; formal analysis, F.G. and Y.Y.; writing—original draft preparation, F.G. and Y.Y.; writing—review and editing, G.G. and F.G.; supervision, G.G.; project administration, G.G.; funding acquisition, G.G. All authors have read and agreed to the published version of the manuscript.

Funding: This research was supported by the Tianshan Talent Training Program [grant number 2023TSYCCX0029] and demonstration project for the promotion of forestry and grass science and technology of the central government [grant number Xin 2024TG02].

Data Availability Statement: The data presented in this study are available on request from the corresponding author.

Conflicts of Interest: The authors declare no conflicts of interest.

References

- Barnosky, A.D.; Matzke, N.; Tomiya, S.; Wogan, G.O.; Swartz, B.; Quental, T.B.; Marshall, C.; McGuire, J.L.; Lindsey, E.L.; Maguire, K.C.; et al. Has the Earth's sixth mass extinction already arrived? *Nature* **2011**, *471*, 51–57. [[CrossRef](#)] [[PubMed](#)]
- Ceballos, G.; Ehrlich, P.R.; Dirzo, R. Biological annihilation via the ongoing sixth mass extinction signaled by vertebrate population losses and declines. *Proc. Natl. Acad. Sci. USA* **2017**, *114*, E6089–E6096. [[CrossRef](#)] [[PubMed](#)]
- Cowie, R.H.; Bouchet, P.; Fontaine, B. The Sixth Mass Extinction: Fact, fiction or speculation? *Biol Rev.* **2022**, *97*, 640–663. [[CrossRef](#)] [[PubMed](#)]
- IPCC. *Climate Change 2021: The Physical Science Basis*; Cambridge University Press: Cambridge, UK, 2021.
- Zhang, Y.; Gao, C.; Qin, H. Prediction of suitable growth area of *Elaeagnus mollis* in Ehanxi province and its response to climate change. *J. Appl Ecol.* **2018**, *29*, 1156–1162. [[CrossRef](#)]
- Zhang, Y.; Huang, D.; Jin, X.; Li, L.Q.; Wang, C.M.; Wang, Y.Y.; Pellissier, L.; Johnson, A.C.; Wu, F.C.; Zhang, X.W. Long-term wetland biomonitoring highlights the differential impact of land use on macroinvertebrate diversity in Dongting Lake in China. *Commun. Earth Environ.* **2024**, *5*, 32. [[CrossRef](#)]
- Carvalho, S.B.; Velo-Anton, G.; Tarroso, P.; Portela, A.P.; Barate, M.; Carranza, S.; Morite, C.; Possingham, H. Spatial conservation prioritization of biodiversity spanning the evolutionary continuum. *Nat Ecol Evol.* **2017**, *1*, 151. [[CrossRef](#)] [[PubMed](#)]
- Fahrig, L. Ecological responses to habitat fragmentation per se. *Annu. Rev. Ecol. Evol. Syst.* **2017**, *48*, 1–23. [[CrossRef](#)]
- Fletcher, R.J., Jr.; Didham, R.K.; Banks-Leite, C.; Barlow, J.; Ewers, R.M.; Rosindell, J.; Holt, R.D.; Gonzalez, A.; Pardini, R.; Damschen, E.I.; et al. Is habitat fragmentation good for biodiversity? *Biol. Conserv.* **2018**, *226*, 9–15. [[CrossRef](#)]
- Alsos, I.G.; Ehrlich, D.; Thuiller, W.; Eidesen, P.B.; Tribsch, A.; Schonswetter, P.; Lagaye, C.; Taberlet, P.; Brochmann, C. Genetic consequences of climate change for northern plants. *Proc. R. Soc. B Biol. Sci.* **2012**, *279*, 2042–2051. [[CrossRef](#)]
- Suggitt, A.J.; Wilson, R.J.; August, T.A.; Beale, C.M.; Bennie, J.J.; Dordolo, A.; Fox, R.; Hopkins, J.J.; B.Isaac, N.J.; Jorieux, P.; et al. *Climate Change Refugia for the Flora and Fauna of England*; Natural England: Sheffield, UK, 2014; 210p. Available online: <https://nora.nerc.ac.uk/id/eprint/E2%80%93t/509452> (accessed on 28 July 2023).
- Heusser, L.E. Rapid oscillations in western North America vegetation and climate during oxygen isotope stage 5 inferred from pollen data from Santa Barbara Basin (Hole893A). *Palaeogeogr. Palaeoclimatol.* **2000**, *161*, 407–421. [[CrossRef](#)]
- Maschinski, J.; Baggs, J.E.; Quintana-Ascencio, P.F.; Menges, E.S. Using population viability analysis to predict the effects of climate change on the extinction risk of an endangered limestone endemic shrub, Arizona cliffrose. *Conserv. Biol.* **2010**, *20*, 218–228. [[CrossRef](#)]
- Pounds, J.A.; Bustamante, M.R.; Coloma, L.A.; Consuegra, J.A.; Fogden, M.P.; Foster, P.N.; Marca, E.L.; Masters, K.L.; Merino-Viteri, A.; Puschendorf, R.; et al. Widespread amphibian extinctions from epidemic disease driven by global warming. *Nature* **2006**, *439*, 161–167. [[CrossRef](#)] [[PubMed](#)]

15. Li, X.H.; Tian, H.D.; Wang, Y.; Li, R.Q.; Song, Z.M.; Zhang, F.C.; Xu, M.; Li, D.M. Vulnerability of 208 endemic orendangered species in China to the effects of climate change. *Reg. Environ. Change* **2013**, *13*, 843–852. [[CrossRef](#)]
16. Buonincontri, M.P.; Bosso, L.; Smeraldo, S.; Chiusano, M.L.; Pasta, S.; Pasquale, G.D. Shedding light on the effects of climate and anthropogenic pressures on the disappearance of *Fagus sylvatica* in the Italian lowlands: Evidence from archaeo-anthracology and spatial analyses. *Sci. Total Environ.* **2023**, *877*, 162893. [[CrossRef](#)] [[PubMed](#)]
17. Wang, Y.; Wang, Z. Change of spermatophyte family diversity in distribution patterns with climate change in China. *Heliyon* **2024**, *10*, e28519. [[CrossRef](#)] [[PubMed](#)]
18. Harris, N.L.; Gibbs, D.A.; Baccini, A.; Birdsey, R.A.; Bruin, S.; Farina, M.; Fatoyinbo, L.; Hansen, M.C.; Herold, M.; Houghton, R.A.; et al. Global maps of twenty-first century forest carbon fluxes. *Nat. Clim. Change* **2021**, *11*, 234–240. [[CrossRef](#)]
19. Hua, F.; Bruijnzeel, L.A.; Meli, P.; A.Martin, P.; Zhang, J.; Nakagawa, S.; Miao, X.R.; Wang, W.Y.; McEvoy, C.; Peña-Arancibia, J.L.; et al. The biodiversity and ecosystem service contributions and trade-offs of forest restoration approaches. *Science* **2022**, *6595*, 839–844. [[CrossRef](#)] [[PubMed](#)]
20. Zhang, X. Ecological geographical characteristics and community problems of wild fruit forest in Yili. *J. Integr. Plant. Biol.* **1973**, *2*, 239–253.
21. Liu, X.; Lin, P.; Zhong, J. An analysis and inquiry into the wild apple trees in Iri. *Arid Zone Resear.* **1993**, *10*, 28–33. [[CrossRef](#)]
22. Chu, J.; Feng, L.; Yang, Y.; Lu, B.; Wang, Q.; Zhou, L.; Wang, J. Damage status of *Prunus armeniaca* population in Tianshan wild fruit forest. *Non-Wood For. Res.* **2022**, *40*, 267–274. [[CrossRef](#)]
23. Jiang, N.; Liu, L.; Li, W.; Guo, C.; Zheng, F.; Wu, M. Effects of grazing on natural regeneration of *Prunus armeniaca* population in Xinjiang. *J. Forest Environ.* **2023**, *43*, 507–515. [[CrossRef](#)]
24. Wang, L. Xinjiang wild apple and Xinjiang wild apricot. *Xinjiang Agric. Sci.* **1989**, *6*, 33–34.
25. Liao, K.; Li, G. Wild almond resources in Xinjiang. *Plant J.* **1995**, *5*, 14–15.
26. Yan, G. Study on the wild fruit trees and its conservation of Tianshan mountain in Xinjiang. *Chin. Wild Plant Resour.* **2001**, *20*, 13–14. [[CrossRef](#)]
27. Tian, Z.P.; Zhuang, L.; Li, J.G.; Xu, Z.Q.; Zhang, L. Relationship between community structure of wild fruit forests and their environment on North-facing slopes of the Iri valley. *Chin. J. Appl. Environ. Biol.* **2011**, *17*, 39–45. [[CrossRef](#)]
28. Meng, Y.X.; Ma, G.; Gao, S.; Nashati, N.; Haerhangbek, G.S.; Chu, J.Y.; Zhou, L. Analysis on plant germplasm resources and protection strategies in wild fruit forest county of western Tianshan mountains. *Heilongjiang Agr. Sci.* **2022**, *11*, 51–56. [[CrossRef](#)]
29. Yan, G.; Xu, Z. Wild fruit tree resources in Tianshan mountain area. *North. Hortic.* **2001**, *1*, 24–27.
30. Wang, L.; Cun, D.; Lin, P.; Xu, Z.; Zhao, Y.; Zhang, H. Types below species of Xinjiang wild apricots. *J. Xinjiang Norm. Univ.* **1997**, *16*, 31–36.
31. Cao, Q.; Ji, Y. Vales and protection of wide amonds Resources Grown in Xinjiang. *Chin. Wild Plant Resour.* **2007**, *26*, 41–42, 46.
32. Zhang, Y.; Feng, T.; Zhang, C.; He, T.M.; Zhang, X.; Liu, Z.; Wang, Y.; Shu, H.; Chen, X. Advances in Research of the *Maus sieversii* (Lebed) Rocm. *Acta Horticult. Sinica* **2009**, *36*, 447–452. [[CrossRef](#)]
33. Lake, T.A.; Briscoe Runquist, R.D.; Moeller, D.A. Predicting range expansion of invasivespecies: Pitfalls and best practices for obtaining biologically realistic projections. *Divers. Distrib.* **2020**, *26*, 1767–1779. [[CrossRef](#)]
34. Liu, C.; Wolter, C.; Xian, W.; Jeschke, J.M. Species distribution models have limited spatial transferability for invasive species. *Ecol. Lett.* **2020**, *23*, 1682–1692. [[CrossRef](#)]
35. Ardestani, E.G.; Ghahfarrokhi, Z.H. Ensemble species distribution modeling of *Salvia hydrangea* under future climate change scenarios in Central Zagros Mountains. *Glob. Ecol. Conserv.* **2021**, *26*, e01488. [[CrossRef](#)]
36. Venne, S.; Currie, D.J. Can habitat suitability estimated from MaxEnt predict colonizations and extinctions? *Divers. Distrib.* **2021**, *27*, 873–886. [[CrossRef](#)]
37. Bosso, L.; Panzuto, R.; Balestrieri, R.; Smeraldo, S.; Chiusano, M.L.; Raffini, F.; Canestrelli, D.; Musco, L.; Gili, C. Integrating citizen science and spatial ecology to inform management and conservation of the Italian seahorses. *Ecol. Inform.* **2024**, *79*, 102402. [[CrossRef](#)]
38. Giné, G.A.F.; Faria, D. Combining species distribution modeling and field surveys to reappraise the geographic distribution and conservation status of the threatened thin-spined porcupine (*Chaetomys subspinosus*). *PLoS ONE* **2018**, *13*, e0207914. [[CrossRef](#)]
39. Guisan, A.; Edwards, T.C.; Hastie, T. Generalized linear and generalized additive models in studies of species distributions: Setting the scene. *Ecol. Lett.* **2002**, *157*, 89–100. [[CrossRef](#)]
40. Lantschner, M.V.; de la Vega, G.; Corley, J.C. Predicting the distribution of harmful species and their natural enemies in agricultural, livestock and forestry systems: An overview. *Int. J. Pest. Manag.* **2019**, *65*, 190–206. [[CrossRef](#)]
41. Thuiller, W.; Araújo, M.B.; Lavorel, S. Generalized models vs. classification tree analysis: Predicting spatial distributions of plant species at different scales. *J. Veg. Sci.* **2003**, *14*, 669–680. [[CrossRef](#)]
42. Stohlgren, T.J.; Ma, P.; Kumar, S.; Rocca, M.; Morisette, J.T.; Jarnevich, C.S.; Benson, N. Ensemble habitat mapping of invasive plant species. *Risk. Anal.* **2010**, *30*, 224–235. [[CrossRef](#)]
43. Luo, M.; Wang, H.; Lv, Z. Evaluating the performance of species distribution models Biomod2 and MaxEnt using the giant panda distribution data. *Chin. J. Appl. Ecol.* **2017**, *28*, 4001–4006. [[CrossRef](#)]
44. Hao, T.; Elith, J.; Guillera-Arroita, G.; Lahoz-Monfort, J.J. A review of evidence about use and performance of species distribution modelling ensembles like BIOMOD. *Divers Distrib.* **2019**, *25*, 839–852. [[CrossRef](#)]

45. Gong, X.; Chen, Y.; Wang, T.; Jiang, X.; Hu, X.; Feng, J. Double-edged effects of climate change on plant invasions: Ecological niche modeling global distributions of two invasive alien plants. *Sci. Total Environ.* **2020**, *740*, 139933. [CrossRef]
46. Lázaro-Lobo, A.; Ramirez-Reyes, C.; Lucardi, R.D.; Ervin, G.N. Multivariate analysis of invasive plant species distributions in southern US forests. *Landsc. Ecol.* **2021**, *36*, 3539–3555. [CrossRef]
47. Zhao, J.; Jiang, C.; Ding, Y.; Li, G.; Li, Q. Potential distribution and disturbance intensity analysis of plateau pika in the source region of the Yellow River via BIOMOD2 integrated model. *Chin. J. Ecol.* **2023**, *43*, 1192–1201.
48. Broennimann, O.; Fitzpatrick, M.C.; Pearman, P.B.; Petitpierre, B.; Pellissier, L.; Yoccoz, N.G.; Thuiller, W.; Fortin, M.J.; Randin, C.; Zimmermann, N.E.; et al. Measuring ecological niche overlap from occurrence and spatial environmental data. *Glob. Ecol. Biogeogr.* **2012**, *21*, 481–497. [CrossRef]
49. Di Cola, V.; Broennimann, O.; Petitpierre, B.; Breiner, F.T.; D’Amen, M.; Randin, C.; Guisan, A. Ecospat: An R package to support spatial analyses and modeling of species niches and distributions. *Ecography* **2017**, *40*, 774–787. [CrossRef]
50. Guisan, A.; Petitpierre, B.; Broennimann, O.; Daehler, C.; Kueffer, C. Unifying niche shift studies: Insights from biological invasions. *Trends Ecol. Evol.* **2014**, *29*, 260–269. [CrossRef]
51. Wang, Y.; Zhao, R.; Zhou, X.; Zhang, X.; Zhao, G.; Zhang, F. Prediction of potential distribution areas and priority protected areas of *Agastache rugosa* based on Maxent model and Marxan model. *Front. Plant Sci.* **2023**, *14*, 1200796. [CrossRef]
52. Xian, X.; Zhao, H.; Wang, R.; Huang, H.; Chen, B.; Zhang, G.; Liu, W.; Wan, F. Climate change has increased the global threats posed by three ragweeds (*Ambrosia* L.) in the Anthropocene. *Sci. Total Environ.* **2023**, *859*, 160252. [CrossRef] [PubMed]
53. Feng, X.; Park, D.S.; Walker, C.; Peterson, A.T.; Merow, C.; Papes, M. A checklist for maximizing reproducibility of ecological niche models. *Nat. Ecol. Evol.* **2019**, *3*, 1382–1395. [CrossRef]
54. Warren, D.L.; Glor, R.E.; Turelli, M. ENMTools: A toolbox for comparative studies of environmental niche models. *Ecography* **2010**, *33*, 607–611. [CrossRef]
55. Dormann, C.G.; Elith, J.; Bacher, S. Collinearity: A review of methods to deal with it and a simulation study evaluating their performance. *Ecography* **2013**, *36*, 27–46. [CrossRef]
56. Thuiller, W.; Georges, D.; Engler, R.; Breiner, F. 'biomod2': Ensemble Platform for Species Distribution Modeling. 2016. Available online: [https://refhub.elsevier.com/S0048-9697\(22\)07352-1/rf202211190900180969](https://refhub.elsevier.com/S0048-9697(22)07352-1/rf202211190900180969) (accessed on 28 July 2023).
57. Zhao, G.; Cui, X.; Sun, J.; Breiner, F. Analysis of the distribution pattern of Chinese *Ziziphus jujuba* under climate change based on optimized biomod2 and MaxEnt models. *Ecol. Indic.* **2021**, *132*, 108256. [CrossRef]
58. Peterson, A.T.; Papes, M.; Soberón, J. Rethinking receiver operating characteristic analysis applications in ecological niche modeling. *Ecol. Model.* **2008**, *213*, 63–72. [CrossRef]
59. Allouche, O.; Tsoar, A.; Kadmon, R. Assessing the accuracy of species distribution models: Prevalence, kappa and the true skill statistic (TSS). *J. Appl. Ecol.* **2006**, *43*, 1223–1232. [CrossRef]
60. Pachauri, R.K.; Allen, M.R.; Barros, V.R.; Broome, J.; Cramer, W.; Christ, R.; Church, J.A.; Clarke, L.; Dahe, Q.; Dasgupta, P.; et al. *Climate Change 2014: Synthesis Report. Contribution of Working Groups I, II and III to the Fifth Assessment Report of the Intergovernmental Panel on Climate Change*; IPCC: Geneva, Switzerland, 2014; p. 151.
61. Brown, J. SDM toolbox: A python-based GIS toolkit for landscape genetic, biogeographic and species distribution model analyses. *Methods Ecol. Evol.* **2014**, *5*, 694–700. [CrossRef]
62. Hamid, M.; Khuroo, A.A.; Charles, B.; Ahmad, R.; Singh, C.P.; Aravind, N.A. Impact of climate change on the distribution range and niche dynamics of Himalayan birch, a typical treeline species in Himalayas. *Biodivers. Conserv.* **2019**, *28*, 2345–2370. [CrossRef]
63. Bosso, L.; Smeraldo, S.; Russo, D.; Chiusano, M.L.; Bertorelle, G.; Johannesson, K.; Roger, K.; Butlin, R.K.; Danovaro, R.; Raffini, F. The rise and fall of an alien: Why the successful colonizer *Littorina saxatilis* failed to invade the Mediterranean Sea. *Biol. Invasions* **2022**, *24*, 3169–3187. [CrossRef]
64. Schoener, T.W. The anolis lizards of bimini: Resource partitioning in a complex fauna. *Ecology* **1968**, *49*, 704–726. [CrossRef]
65. Li, H.; Tan, W.; Li, T. Study on the protection pattern of biological and cultural diversity in Pu ‘er “Tea-horse ancient road”. *Chin. Landsc. Archit.* **2019**, *35*, 46–51. [CrossRef]
66. Xie, W.; Jia, J.; Bu, C.; Ma, L.; Guo, J.; Song, K.; Li, X.; Sun, Y.; Fang, Y. Habitat assessment of birds under national key protection in Yanshan area and analysis of conservation gap of national nature reserve. *Chin. J. Zool.* **2022**, *57*, 170–184. [CrossRef]
67. Zhang, L.; Ouyang, Z.; Xiao, Y.; Xu, W.; Zhang, H.; Jiang, B. Evaluation and systematic conservation planning of biodiversity conservation priority area in Hainan island. *J. Appl. Ecol.* **2011**, *22*, 2105–2112. [CrossRef]
68. Mou, X.; Rao, S.; Zhang, X.; Wang, X.; Zhu, Z. Evaluation of county biodiversity conservation priority pattern and optimization of conservation system: A case study of Wuyishan city. *J. Ecol. Rural.* **2021**, *37*, 769–777. [CrossRef]
69. Abdulwahab, U.A.; Hammill, E.; Hawkins, C.P. Choice of climate data affects the performance and interpretation of species distribution models. *Ecol. Model.* **2022**, *471*, 110042. [CrossRef]
70. Sugalski, M.T.; Claussen, D.L. Preference for soil moisture, soil pH, and light intensity by the salamander, *Plethodon cinereus*. *Afr. J. Herpetol.* **1997**, *31*, 245–250. [CrossRef]
71. Townsend Peterson, A.; Papes, M.; Eaton, M. Transferability and model evaluation in ecological niche modeling: A comparison of GARP and maxent. *Ecography* **2007**, *30*, 550–560. [CrossRef]
72. González, M.P.; Diez, J.M.; Ibáñez, I.; Font, X.; Vilà, M. Plant invasions are context-dependent: Multiscale effects of climate, human activity and habitat. *Divers. Distrib.* **2014**, *20*, 720–731. [CrossRef]

73. Aalto, J.; Luoto, M. Integrating climate and local factors for geomorphological distribution models. *Earth Surf. Proc. Land.* **2014**, *39*, 1729–1740. [[CrossRef](#)]
74. Ma, X.Y.; Xu, H.; Cao, Z.Y.; Shu, L.; Zhu, R.L. Will climate change cause the global peatland to expand or contract? Evidence from the habitat shift pattern of *Sphagnum mosses*. *Glob. Change Biol.* **2022**, *28*, 6419–6432. [[CrossRef](#)]
75. Urban, M.C.; Tewksbury, J.J.; Sheldon, K.S. On a collision course: Competition and dispersal differences create no-analogue communities and cause extinctions during climate change. *Proc. R. Soc. B Biol. Sci.* **2012**, *279*, 2072–2080. [[CrossRef](#)]
76. Blois, J.L.; Zarnetske, P.L.; Fitzpatrick, M.C.; Finnegan, S. Climate change and the past, present, and future of biotic interactions. *Science* **2012**, *341*, 499–504. [[CrossRef](#)]
77. Midgley, G.F.; Hannah, L.; Millar, D.; Rutherford, M.C.; Powrie, L.W. Assessing the vulnerability of species richness to anthropogenic climate change in a biodiversity hotspot. *Glob. Ecol. Biogeogr.* **2002**, *11*, 445–451. [[CrossRef](#)]
78. Sommer, J.H.; Kreft, H.; Kier, G.; Jetz, W.; Mutke, J.; Barthlott, W. Projected impacts of climate change on regional capacities for global plant species richness. *Proc. R. Soc. B Biol. Sci.* **2010**, *277*, 2271–2280. [[CrossRef](#)]
79. Tian, Z. The Patterns and Drivers of Wild Fruit Tree Species Diversity in the Ili Valley of Xinjiang, China. Ph.D. Thesis, East China Normal University, Shanghai, China, 2023. [[CrossRef](#)]
80. Tian, Z.; Song, H.; Wang, Y.; Li, J.; Maimaiti, M.; Liu, Z.; Zhang, H.X.; Zhang, J. Wild apples are not that wild: Conservation status and potential threats of *Malus sieversii* in the mountains of Central Asia biodiversity hotspot. *Diversity* **2022**, *14*, 489. [[CrossRef](#)]
81. Feeley, K.J.; Silman, M.R.; Bush, M.B.; Farfan, W.; Cabrera, K.G.; Malhi, Y.; Meir, P.; Revilla, N.S.; Quisiyupanqui, M.N.R.; Saatchi, S. Upslope migration of Andean trees. *J. Biogeogr.* **2011**, *38*, 783–791. [[CrossRef](#)]
82. Corlett, R.T.; Westcott, D.A. Will plant movements keep up with climate change? *Trends Ecol. Evol.* **2013**, *28*, 482–488. [[CrossRef](#)]
83. Delzon, S.; Urli, M.; Samalens, J.C.; Lamy, J.B.; Lischke, H.; Sin, F.; Zimmermann, N.E.; Porte, A.J. Field evidence of colonisation by holm oak, at the northern margin of its distribution range, during the anthropocene period. *PLoS ONE* **2013**, *8*, e80443. [[CrossRef](#)]
84. Steinbauer, M.J.; Grytnes, J.A.; Jurasinski, G.; Kulonen, A.; Lenoir, J.; Pauli, H.; Rixen, C.; Winkler, M.; Bardy-Durchhalter, M.; Barni, E.; et al. Accelerated increase in plant species richness on mountain summits is linked to warming. *Nature* **2018**, *556*, 231–234. [[CrossRef](#)]
85. Parmesan, C.; Yohe, G. A globally coherent fingerprint of climate change impacts across natural systems. *Nature* **2003**, *421*, 37–42. [[CrossRef](#)]
86. Chen, I.C.; Hill, J.K.; Ohlemüller, R.; Roy, D.B.; Thomas, C.D. Rapid range shifts of species associated with high levels of climate warming. *Science* **2011**, *333*, 1024–1026. [[CrossRef](#)]
87. Liu, H.; Guan, K.; Zhang, D.; Zhang, Y. Protection of degraded Wild Fruit Forest in Tianshan Mountains. *Oryx* **2023**, *57*, 699–700. [[CrossRef](#)]
88. Bettoni, J.C.; Bonnart, R.; Volk, G.M. Challenges in implementing plant shoot tip cryopreservation technologies. *Plant Cell Tissue Organ Cult.* **2021**, *144*, 21–34. [[CrossRef](#)]
89. Bramel, P.J.; Volk, G.M. *A Global Strategy for the Conservation and Use of Apple Genetic Resources*; Glob Crop Diversity Trust: Bonn, Germany, 2019. [[CrossRef](#)]
90. Wang, Q.; Zhang, Z.; Du, R.; Wang, S.; Duan, J.; Iler, A.M.; Piao, S.; Luo, C.; Jiang, L.; Lv, W.W.; et al. Richness of plant communities plays a larger role than climate in determining responses of species richness to climate change. *J. Ecol.* **2019**, *107*, 1944–1955. [[CrossRef](#)]
91. Zhang, Y.F.; Dang, Y.Q.; Wang, X.Y. Risk analysis of dispersal and outbreak of *Massicus raddei* (Coleoptera: Cerambycidae) in China based on climate and host distribution. *Scientia Silvae Sinicae* **2022**, *58*, 95–109. [[CrossRef](#)]
92. Xu, D.; Gao, J.; Lin, W.; Zhou, W. Differences in the ecological impact of climate change and urbanization. *Urban Clim.* **2021**, *38*, 100891. [[CrossRef](#)]
93. Dri, G.F.; Fontana, C.S.; Dambros, C. Estimating the impacts of habitat loss induced by urbanization on bird local extinctions. *Biol. Conserv.* **2021**, *256*, 109064. [[CrossRef](#)]
94. Han, L.; Zhang, Z.; Tu, W.; Zhang, Q.; Hong, Y.; Chen, S.; Lin, Z.Q.; Gu, S.; Du, Y.B.; Wu, Z.J.; et al. Preferred prey reduce species realized niche shift and improve range expansion prediction. *Sci. Total Environ.* **2023**, *859*, 160370. [[CrossRef](#)]
95. Miller, J.R.; Turner, M.G.; Smithwick, E.A.; Dent, C.L.; Stanley, E.H. Spatial extrapolation: The science of predicting ecological patterns and processes. *BioScience* **2004**, *54*, 310–320. [[CrossRef](#)]
96. Sheth, S.N.; Angert, A.L. The evolution of environmental tolerance and range size: A comparison of geographically restricted and widespread *Mimulus*. *Evolution* **2014**, *68*, 2917–2931. [[CrossRef](#)]

Disclaimer/Publisher’s Note: The statements, opinions and data contained in all publications are solely those of the individual author(s) and contributor(s) and not of MDPI and/or the editor(s). MDPI and/or the editor(s) disclaim responsibility for any injury to people or property resulting from any ideas, methods, instructions or products referred to in the content.